08_54

ELSEVIER

Discrete Applied Mathematics 105 (2000) 1–38

DISCRETE APPLIED MATHEMATICS

Symmetric patterns in the cellular automaton that generates Pascal's triangle modulo 2

André Barbé

Department of Electrical Engineering, Katholieke Universiteit Leuven, Kardinaal Mercierlaan, 94, B-3001 Leuven/Belgium

Received 1 March 1999; revised 3 December 1999; accepted 13 March 2000

Abstract

A *binary difference pattern* (BDP) is a pattern obtained by covering an equilateral triangular grid by black and white circles in a dense hexagonal packing under a simple symmetric local matching rule. It is a subpattern in a specific graphical representation of the orbit of a cellular automaton that generates Pascal's triangle modulo 2. Analytic conditions for certain types of geometric symmetry of these patterns are derived. These allow us to find all symmetric solutions and the cardinalities of the different symmetry classes. In the analysis, a central role is played by the so-called *Pascal matrix* — a square matrix that contains Pascal's triangle modulo 2 (up to a certain size) — and by certain groups of geometric transformations of this matrix, featuring remarkable product properties for the Pascal matrix. © 2000 Elsevier Science B.V. All rights reserved.

Keywords: Symmetric arrangements; Local matching; Pascal's triangle; Pascal matrix; Cellular automata; Tetrahedron coverings

1. Introduction

Let S be a finite set, then $\underline{s} \stackrel{\text{def}}{=} (s(k))_{k\in\mathbb{Z}} \in S^{\mathbb{Z}}$ represents a one-dimensional bidirectional sequence with values in S. A one-dimensional cellular automaton (CA) can be considered as a discrete dynamical system defined by the recursive mapping $A: S^{\mathbb{Z}} \to S^{\mathbb{Z}} : (A\underline{s})(k) = \phi(s(k+j_1), s(k+j_2), \ldots, s(k+j_M))$, $j_1, j_2, \ldots, j_M \in \mathbb{Z}$, where ϕ is a mapping from $S^M \to S$, known as the *local evolution rule* of the automaton. The CA starts in an *initial state* $\underline{s}_0 \in S^{\mathbb{Z}}$. The state at "time" r is given by $\underline{s}_r = A^r \underline{s}_0$.

E-mail address: andre.barbe@esat.kuleuven.ac.be (A. Barbé).

0166-218X/00/$ - see front matter © 2000 Elsevier Science B.V. All rights reserved.
PII: S0166-218X(00)00211-0

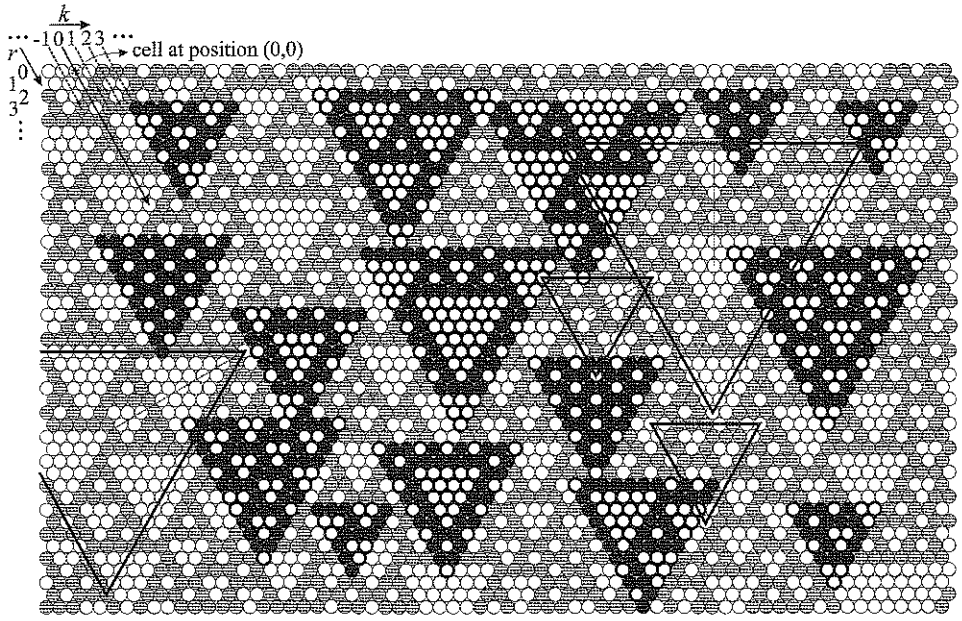


Fig. 1. An orbit of the binary-valued cellular automaton with local evolution rule $\phi(s(k),s(k+1))=(s(k)+s(k+1)) \bmod 2$ and with a random initial state (top row). A white cell has state-value 0, a grey or black cell has state-value 1. The highlighted equilateral triangular clusters (*binary difference patterns*) display either reflective, rotational or full dihedral (D_3) symmetry (involving rotations of 120°). A few additional symmetric clusters are also indicated by a triangle running over the boundary cells.

The two-dimensional sequence $O_A(\underline{s}_0) \stackrel{\text{def}}{=} (A^r \underline{s}_0)_{r\in\mathbb{N}}$ is called *the orbit* of the CA and represents the global state-time evolution of the CA. Cellular automata studies are mainly concerned with the properties of such orbits, which are generally displayed in an appropriate graphical form (see for example [19,13]).

In this paper, we restrict our attention to certain patterns in the orbit of the two-valued additive (linear) CA defined on $S=\mathbb{F}_2$ (the finite field with elements 0 and 1), with local rule $\phi(s(k),s(k+1))=(s(k)+s(k+1)) \bmod 2$. Fig. 1 shows a graphical representation of a part of this CA's orbit produced from a random initial state. Each element $O_A(\underline{s}_0)(r,k)$ of the orbit is represented by a circular "cell": the cell is white when the element has value 0, it is gray or black when the element has value 1. The cell-coordinate (r,k) is defined with respect to the particular skew coordinate system as displayed in the figure. The graphical representation of the orbit generated from an initial state $\underline{s}_0=\underline{\delta}_{k_0}$, such that for a given $k_0 \in \mathbb{Z}$: $\delta_{k_0}(k_0)=1$ and $\delta_{k_0}(k)=0$ when $k \neq k_0$, is known to display a pattern that is isomorphic to *Pascal's triangle modulo* 2 (see [16]). Part of this pattern is shown in Fig. 2: it will be referred to as the *Pascal triangle pattern* (PTP). Because of the additivity of the local CA-rule ϕ in focus here, the orbit pattern in Fig. 1 can actually be considered as the cellwise addition modulo 2 of all PTPs generated from the black cells on its top row. Pascal's triangle and related patterns in CA have been subject of several studies, see for example [1,2,15].

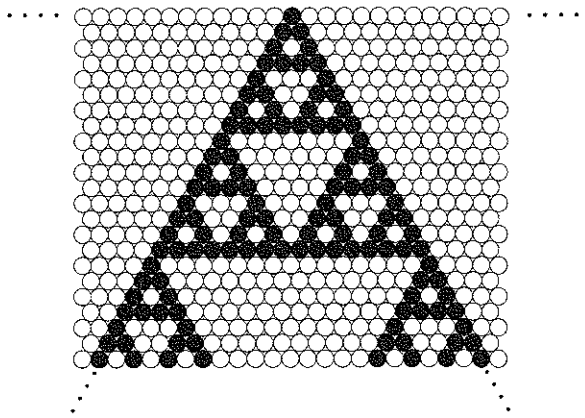


Fig. 2. The Pascal triangle pattern (PTP): it is the BDP of an infinite sequence with only one black cell in its top row configuration, and is in 1–1 correspondence with Pascal's triangle mod 2.

We have highlighted several clusters of cells in the orbit of Fig. 1: those consisting of black cells and of white cells having a thicker boundary line. All these clusters are confined in a top-down equilateral triangular shape and display — as a pattern — distinct symmetries. Thus, reflection symmetries, rotational symmetry, and full equilateral triangle (dihedral) symmetry can be discovered. Moreover, the content of any top-down equilateral triangular cluster in this orbit (not only the ones featuring a symmetric pattern) is completely determined by the cell states of its top-edge. Such triangular cluster — earlier called the *binary difference field* associated with the given top-edge sequence [4,5] — is called a *binary difference pattern* (BDP) in the present context (see also further).

This paper investigates symmetries in BDPs. As such, symmetric BDPs also form an extension of a class of complex pattern generating mechanisms which also enforce a *global* condition on patterns which are generated by applying a local CA-mechanism (see [4–7,9]). Here, the global condition is clearly a symmetry condition.

Now follows a short overview of the paper's content.

Central in the analysis is the so-called *Pascal matrix*: a square matrix that features Pascal's triangle modulo 2 (up to some finite size), and all its transformations under the rotations and reflections that leave a square invariant (forming the dihedral group D_4). Consequently, these transformations as well as the Pascal matrix [1] are discussed in the preliminary Section 2.

Section 3 introduces the binary difference pattern (BDP) generated by a binary string, and shows that it can be considered as a composition of shifted versions of a geometric representation of Pascal's triangle modulo 2. The invariance of the BDP-nature of a BDP under certain geometric operations (forming a dihedral D_3-group), together

[1] To the author's knowledge, Pascal matrices are not frequently met in mathematics, in contrast with Pascal's triangle. Referees of this paper pointed, for example, to papers [11,20] in which a Pascal matrix appears, be it in a totally different context.

with the analytic relationship between the three edge-sequences of a BDP, uncovers a D_3-group property among four of the eight transforms of the Pascal matrix (when completed with the identity matrix and the vertical reflection of the identity matrix, and with the ordinary matrix product modulo 2 as the related binary operation).

Section 4 looks for BDPs with palindromic, rotational and dihedral symmetry. Analytic conditions for these symmetries and the cardinalities of the corresponding symmetry classes are derived.

In Section 5, we introduce a second type of BDP-covering of an equilateral triangle, producing the so-called $\triangle$-BDPs. These can also be considered as a superposition of Pascal's triangles modulo 2. The $\triangle$-BDP properties uncover a D_3-group property among the four transforms of the Pascal matrix that remained unused before (again after extension with the identity matrix and its vertical reflection, and under matrix multiplication modulo 2).

In Section 6, we derive and solve the analytic conditions under which a $\triangle$-BDP exhibits certain geometric symmetries.

The final Section 7 shows how the results of the previous sections can be used to construct a regular tetrahedron in which the four faces are BDPs or $\triangle$-BDPs, under the requirement that they match along the edges of the tetrahedron. Some of the polyhedral coverings of Escher, and the Kaleidocycles of Schattschneider and Wallace based on Escher's drawings (see for example [17,18]), have been influential in considering this kind of application.

2. Preliminaries: D_4^G-operations on matrices, Pascal matrix

Let A be a square matrix (of size N), with elements $A(m,n)$, $m,n=0,1,\ldots,N-1$. (m indicates the row address, n the column address). In what follows, we will consider all transformations of A under the eight geometric operations (rotations and reflections) that leave a square invariant. These operations form the dihedral group D_4^G under their usual composition, denoted by $\circ$:

$$D_4^G = \langle 0, <, \vee, >, \uparrow, \rightarrow, \nearrow, \searrow; \circ \rangle,$$

where the first four elements (pronounced as 0, left-vee, vee, right-vee, respectively) denote the *counterclockwise* rotations of $0^\circ, 90^\circ, 180^\circ$ and 270°, respectively; the last four elements [pronounced as up, right, rup (from right-up), rown (from right-down)] denote the reflections about a line that is *perpendicular* to the direction indicated by the arrows (for example, $\uparrow$ represents a reflection about a horizontal line, $\nearrow$ represents a reflection about the \-diagonal). We have used the superscript G in D_4^G, in order to stress the geometric character of the operations and to distinguish it from the isomorphic "abstract" dihedral group D_4.

If a square matrix A is transformed by applying one of these operations, we indicate this by a superscript that corresponds to that operation: $A^0(\equiv A), A^>, A^\vee, A^>, A^\uparrow, A^\rightarrow, A^\nearrow, A^\searrow$. For example, $A^\nearrow$ (pronounced "A-rup") corresponds to the usual transpose of A,

while $A^{<}$ (pronounced "A left-vee") rotates the matrix A counterclockwise by 90°. If different operations are applied in sequence, e.g., first $\uparrow$, followed by a rotation of 180° ($\vee$), then we write $(A^{\uparrow})^{\vee}$.

Combinations of operations always correspond to a single operation, according to the well-known Cayley-table of the D_4^G-group (see for example [12]), which we display here for further easy reference with the symbols just introduced. (Convention: with x and y two elements from the group, $(A^x)^y = A^{(y \circ x)}$, where $y \circ x$ is found on the intersection of row y and column x.)

$\circ$	0	$\vee$	$\uparrow$	$\rightarrow$	$<$	$>$	$\nearrow$	$\searrow$
0	0	$\vee$	$\uparrow$	$\rightarrow$	$<$	$>$	$\nearrow$	$\searrow$
$\vee$	$\vee$	0	$\rightarrow$	$\uparrow$	$>$	$<$	$\searrow$	$\nearrow$
$\uparrow$	$\uparrow$	$\rightarrow$	0	$\vee$	$\nearrow$	$\searrow$	$<$	$>$
$\rightarrow$	$\rightarrow$	$\uparrow$	$\vee$	0	$\searrow$	$\nearrow$	$>$	$<$
$<$	$<$	$>$	$\searrow$	$\nearrow$	$\vee$	0	$\uparrow$	$\rightarrow$
$>$	$>$	$<$	$\nearrow$	$\searrow$	0	$\vee$	$\rightarrow$	$\uparrow$
$\nearrow$	$\nearrow$	$\searrow$	$>$	$<$	$\rightarrow$	$\uparrow$	0	$\vee$
$\searrow$	$\searrow$	$\nearrow$	$<$	$>$	$\uparrow$	$\rightarrow$	$\vee$	0

(1)

Let $\boldsymbol{v}$ be a column vector (of size N) with components $v(0), \ldots, v(N-1)$. $\boldsymbol{v}^{\uparrow}$ is the vector that shows the elements of $\boldsymbol{v}$ in reverse order: $v^{\uparrow}(m) = v(N-1-m)$, $m = 0, \ldots, N-1$.

The next properties concerning D_4^G-operations on matrix products follow directly from these definitions and from the definition of the matrix product.

Lemma 1. *Let A, B be two square matrices, I the identity matrix, and $\boldsymbol{v}$ a vector (all of size N), then the following relations hold:*

$$\begin{array}{lll}
\text{(a) } AB = A^{\rightarrow}B^{\uparrow}, & \text{(b) } (AB)^{<} = B^{<}A^{\nearrow}, & \text{(c) } (AB)^{\vee} = A^{\uparrow}B^{\rightarrow}, \\
\text{(d) } (AB)^{>} = B^{\nearrow}A^{>}, & \text{(e) } (AB)^{\uparrow} = A^{\uparrow}B, & \text{(f) } (AB)^{\rightarrow} = AB^{\rightarrow}, \\
\text{(g) } (AB)^{\nearrow} = B^{\nearrow}A^{\nearrow}, & \text{(h) } (AB)^{\searrow} = B^{<}A^{>}, & \\
\text{(i) } I^{\uparrow} = I^{\rightarrow}, & \text{(j) } (I^{\uparrow})^2 = I, & \text{(k) } (I^{\uparrow})^{-1} = I^{\uparrow}. \\
\text{(l) } \boldsymbol{v}^{\uparrow} = I^{\uparrow}\boldsymbol{v}, & \text{(m) } A^{\rightarrow}\boldsymbol{v}^{\uparrow} = A\boldsymbol{v}, &
\end{array} \tag{2}$$

Observe that, in this table of equalities, if $z \in R \stackrel{\text{def}}{=} \langle 0, \vee, \uparrow, \rightarrow \rangle$ — the Abelian normal subgroup of D_4^G formed by the operations that leave a rectangle invariant — then $(AB)^z = A^x B^y$, where x and y also belong to this subgroup. On the other hand, if z is one of the four remaining operations: $z \in \bar{R} \stackrel{\text{def}}{=} D_4^G \setminus R = \{<, >, \nearrow, \searrow\}$ (which do not form a group), then $(AB)^z = B^x A^y$, with $x, y \in \bar{R}$ (notice the reversal of A and B here). Thus, there is a kind of natural separation in the D_4^G-operations in relation to matrix products. This separation will reappear in Sections 3 and 5 in a different context, where the operations are applied on a particular matrix that will play a central role in what follows. We define this matrix now.

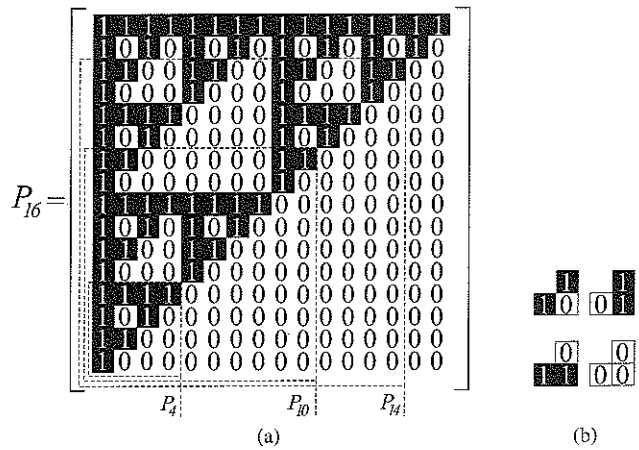


Fig. 3. P_{16}: (a) Pascal matrix modulo 2 of size 16. Pascal matrices of smaller size are submatrices of P_{16}, as indicated. Extensions to higher sizes are trivial: a new row can be put on top of P_N by letting it start with a 1 on column 0 and end with a 1 on column N; the intermediate elements of the new row are formed by applying the local configuration rule shown under (b).

Definition 1. P_N, the *Pascal matrix* modulo 2 of size N, is the square $N \times N$ matrix with elements $p_N(m,n)$, $m,n = 0,1,\ldots,N-1$:

$$p_N(m,n) = \begin{cases} \binom{N-m-1}{n} \bmod 2 & \text{for } n \leqslant N-1-m, \\ 0 & \text{for } n > N-1-m. \end{cases} \tag{3}$$

Remark 1. P_N is the square matrix of size N whose upper-left triangular part is Pascal's triangle modulo 2 (see for example [16]), placed upside-down, as shown in Fig. 3. The other elements are all 0.

Note that, because of its left upper-triangular structure with an upward diagonal that has a 1 everywhere, P_N has full rank in $\mathbb{F}_2$, the field of integers mod 2 (with elements 1 and 0). Actually, all P_N-transforms have full rank for a similar reason. Thus, the following proposition is true:

Lemma 2. *P_N and all its transforms are invertible in $\mathbb{F}_2$.*

3. The difference pattern of a binary string and Pascal's triangle modulo 2

3.1. The binary difference pattern

Consider a finite binary *sequence* or *string* of length N, with elements in $\mathbb{F}_2$:

$$\boldsymbol{a}_N = a(0)a(1)a(2)\ldots a(N-1).$$

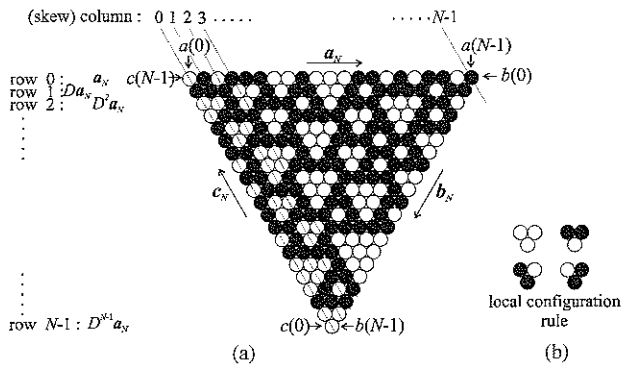


Fig. 4. (a) The binary difference pattern of the binary sequence $\boldsymbol{a}_N$. (b) The only possible local configurations.

Depending on the context, $\boldsymbol{a}_N$ will also be interpreted as a column vector with components $a(0), a(1), \ldots, a(N-1)$.

Definition 2. The nth-order *difference sequence* of $\boldsymbol{a}_N$, denoted by $D_n\boldsymbol{a}_N$ $(n \leqslant N-1)$ is defined by the recursion

$$D_{n+1}\boldsymbol{a}_N = D(D_n\boldsymbol{a}_N), \tag{4}$$

where $D\boldsymbol{a}_N = D_1\boldsymbol{a}_N$ is the sequence of length $N-1$ given by

$$D\boldsymbol{a}_N(k) = (a(k) + a(k+1)) \bmod 2, \quad 0 \leqslant k \leqslant N-1. \tag{5}$$

Note that $a + b \equiv a - b \pmod 2$, hence the name "difference sequence" [4,5]. These difference sequences can be represented as a geometric pattern of black and white circles (*cells*) arranged in a dense hexagonal packing on an equilateral triangular support, as shown in Fig. 4. The top row of cells is in 1–1 correspondence with the elements $a(0), a(1), \ldots, a(N-1)$, from left to right. A black cell corresponds to an a_N-element whose value is 1, a white cell to an element with value 0. When numbering the rows of cells top-downwards, starting from 0, with the top row representing $\boldsymbol{a}_N$, row n corresponds to $D_n\boldsymbol{a}_N$. The sequence at the right edge of the triangle will be denoted by $\boldsymbol{b}_N$ (downward orientation), the left-edge sequence by $\boldsymbol{c}_N$ (upward orientation). Depending on the context, $\boldsymbol{b}_N$ and $\boldsymbol{c}_N$ may be interpreted as vectors. Introducing a (skew)-column ranking from 0 to $N-1$, as indicated in Fig. 4, and representing the state of the cell at row m and column n as $d(m,n)$, this *binary difference pattern* (BDP) can also be interpreted as the *finite* orbit of a cellular automaton [4,5,9,16,19] with *finite* initial configuration $\boldsymbol{a}_N$ under the local evolution rule

$$d(m,n) = (d(m-1,n) + d(m-1,n+1)) \bmod 2. \tag{6}$$

This implies the *local geometric configuration rule* shown in Fig. 4(b), which is present all over the pattern. Observe that this rule (the set of local configurations shown in Fig. 4(b)) exhibits the symmetry of an equilateral triangle (dihedral symmetry D_3; [10]): it is invariant under rotations by $0^\circ, 120^\circ$ and 240°, and also under reflections

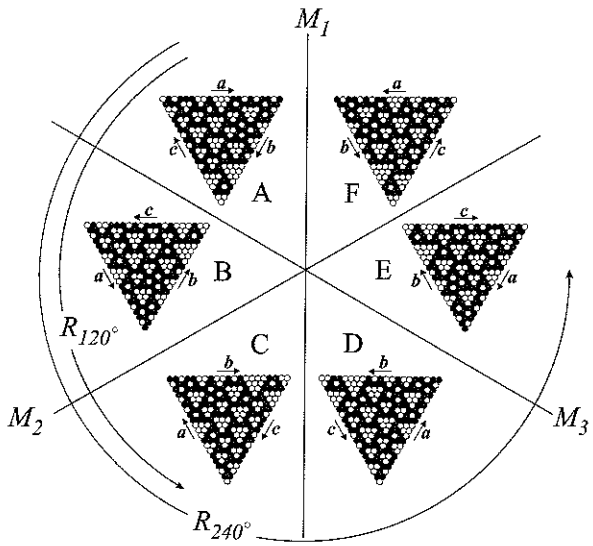


Fig. 5. The transformations of an original Binary Difference Pattern (A) under the rotations $R_{120°}$, $R_{240°}$ and under the median reflections M_1, M_2, M_3. The BDP-character remains invariant under these operations (and under all compositions thereof). Patterns A, C, E and B, D, F are linked through the rotations. Adjacent and opposite configurations are reflections about one of the median axes M_1, M_2, M_3.

about the medians of the "triangular" local configuration patterns. And so does the BDP as a whole: it remains a BDP under rotations by $0°, 120°$ and $240°$, and also under reflections about the medians M_1, M_2, M_3. This is represented in Fig. 5, using the notations $R_{120°}, R_{240°}$ for the (counterclockwise) rotations, and M_1, M_2, M_3 for both the medians and the corresponding reflection operations. If we denote the BDPs shown in this figure by A, B, C, D, E, F, then the results of applying e.g. $R_{240°}$ to A, denoted by $R_{240°}(A)$, equals E. In the same way, we find $R_{0°}(A)=A$, $R_{120°}(A)=C$, $R_{240°}(A)=E$, $M_1(A)=F$, $M_2(A)=D$, $M_3(A)=B$. The figure directly shows how these operations act on any of the other BDPs as well: e.g. $M_2(C)=B$, $R_{240°}(B)=F$, etc. We will further refer to the well-known fact that this set of operations forms, under the usual composition of these operations, the dihedral group

$$D_3^G = \langle R_{0°},\ R_{120°},\ R_{240°},\ M_1,\ M_2,\ M_3; \circ \rangle.$$

For further easy reference, we display its Cayley-table:

$\circ$	$R_{0°}$	$R_{120°}$	$R_{240°}$	M_1	M_2	M_3
$R_{0°}$	$R_{0°}$	$R_{120°}$	$R_{240°}$	M_1	M_2	M_3
$R_{120°}$	$R_{120°}$	$R_{240°}$	$R_{0°}$	M_3	M_1	M_2
$R_{240°}$	$R_{240°}$	$R_{0°}$	$R_{120°}$	M_2	M_3	M_1
M_1	M_1	M_2	M_3	$R_{0°}$	$R_{120°}$	$R_{240°}$
M_2	M_2	M_3	M_1	$R_{240°}$	$R_{0°}$	$R_{120°}$
M_3	M_3	M_1	M_2	$R_{120°}$	$R_{240°}$	$R_{0°}$

(7)

(the convention used: $y \circ x$ means applying x first, then y; $y \circ x$ is found in the Cayley-table on the intersection of row y and column x).

It can readily be checked, using Fig. 5, that if $g,\ h \in D_3^G$, then $(h \circ g)(A) = h(g(A))$, no matter what the particular nature of the BDP A is. This observation allows us to state formally that the mapping

$$\phi_{G,\mathscr{B}} : D_3^G \times \mathscr{B} \to \mathscr{B} : (g, X) \mapsto g(X) \tag{8}$$

defines an *action* [14,3] of the group D_3^G on the set $\mathscr{B}$ of all BDPs (of size N). The BDP-set

$$\mathscr{U} = \{A, B, C, D, E, F\}$$

is then the *orbit* of any of its members under the action of D_3^G, and Fig. 5 actually illustrates the action $\phi_{G,\mathscr{U}} : D_3^G \times \mathscr{U} \to \mathscr{U}$. Later, BDPs in the same orbit will be considered indistinguishable.

The edge-sequences of the original BDP A in Fig. 5 are represented by $\boldsymbol{a}, \boldsymbol{b}, \boldsymbol{c}$. These sequences are read in clockwise sense. Under median-reflection, the orientation of the edge-sequences reverses, as indicated by the arrows. Reading the reversed sequences in clockwise sense produces $\boldsymbol{a}^{\uparrow}, \boldsymbol{b}^{\uparrow}, \boldsymbol{c}^{\uparrow}$.

Let us denote the symbolic substitution $\boldsymbol{a} \mapsto \boldsymbol{x}$, $\boldsymbol{b} \mapsto \boldsymbol{y}$, $\boldsymbol{c} \mapsto \boldsymbol{z}$ by σ_{xyz}. Then, the invariance of the BDP-nature under the D_3^G-operations implies that all relationships that might exist between the edge-sequences $\boldsymbol{a}, \boldsymbol{b}, \boldsymbol{c}$ remain valid under the symbolic substitutions $\sigma_{abc}, \sigma_{a^{\uparrow}c^{\uparrow}b^{\uparrow}}, \sigma_{cab}, \sigma_{b^{\uparrow}a^{\uparrow}c^{\uparrow}}, \sigma_{bca}, \sigma_{c^{\uparrow}b^{\uparrow}a^{\uparrow}}$ (applying these substitutions to $(\boldsymbol{a}, \boldsymbol{b}, \boldsymbol{c})$ corresponds to renaming the top-edge, right-edge and left-edge sequences as indicated in the transformed figures A, B, C, D, E, F in Fig. 5, respectively).

From the linearity of the binary difference rule (5), it follows that the BDP of a given sequence is obtained from the cellwise addition modulo 2 of the Pascal triangle patterns (recall Fig. 2) that propagate from all the black cells in that given sequence, thereby restricting these patterns to the triangular BDP-support of the sequence.

We are interested in finding BDPs that satisfy certain symmetry conditions. For example: what are the BDPs for which the three edge-sequences are equal? In order to answer questions of this kind, we need to express the dependence between these edge-sequences.

It is not difficult to show, using (6) iteratively a proper number of times, that any cell $d(m,n)$ in the BDP can be written as dependent on the states of certain cells on an arbitrary row $(m-r)$ above this cell, (r fixed, $1 \leqslant r \leqslant m$):

$$d(m,n) = \sum_{k=0}^{r} \rho(r,k) d(m-r, n+k) \bmod 2, \tag{9}$$

where

$$\rho(r,k) \stackrel{\text{def}}{=} \binom{r}{k} \bmod 2. \tag{10}$$

Returning to Fig. 4, we can now relate the elements of the left-edge sequence $\boldsymbol{c}_N$ to the elements of the top-edge sequence $\boldsymbol{a}_N$, using relationships (9)–(10). Indeed,

$$c(m) = d(N-m-1,0) \overset{(9)}{=} \sum_{k=0}^{N-m-1} \rho(N-m-1,k)d(0,k) \bmod 2$$
$$\overset{(10)}{=} \sum_{k=0}^{N-m-1} \binom{N-m-1}{k} a(k) \bmod 2. \tag{11}$$

Considering the $c(m)$, $m = 0,\ldots,N-1$ as components of the vector $\boldsymbol{c}_N$ and invoking the definition of the Pascal matrix P_N, we find that (11) is equivalent to

$$\boldsymbol{c}_N = P_N \boldsymbol{a}_N \,(\mathrm{mod}\, 2). \tag{12}$$

Recall that all arithmetic is done modulo 2. This will no longer be explicitly indicated. When the context is clear, we will also delete the size-indicating subscript N, since the relationship holds for all $N \geqslant 1$. Because a given BDP remains a BDP under the D_3^G-operations, relationship (12) also holds for the left-edge/top-edge sequences of all BDPs A, B, C, D, E, F that are shown in Fig. 5. We summarize this in

Lemma 3.

$$\begin{array}{lll} \text{(a)} \quad \boldsymbol{c} = P\boldsymbol{a}, & \text{(b)} \ \boldsymbol{a} = P\boldsymbol{b}, & \text{(c)} \ \boldsymbol{b} = P\boldsymbol{c}, \\ \text{(d)} \quad \boldsymbol{b}^{\uparrow} = P\boldsymbol{a}^{\uparrow}, & \text{(d)} \ \boldsymbol{a}^{\uparrow} = P\boldsymbol{c}^{\uparrow}, & \text{(e)} \ \boldsymbol{c}^{\uparrow} = P\boldsymbol{b}^{\uparrow}. \end{array} \tag{13}$$

Lemma 3 represents an algebraic relationship between some pairs of the set $\mathscr{T} \overset{\text{def}}{=} \{\boldsymbol{a}, \boldsymbol{a}^{\uparrow}, \boldsymbol{b}, \boldsymbol{b}^{\uparrow}, \boldsymbol{c}, \boldsymbol{c}^{\uparrow}\}$, where we have to keep in mind that this is a set of edge-sequences of BDPs which are "geometrically" related as shown in Fig. 5. We will now derive similar relationships for all pairs of elements in $\mathscr{T}$.

Property 1. *Let $\boldsymbol{x}, \boldsymbol{y} \in \mathscr{T}$. Then $\boldsymbol{y} = A(\boldsymbol{y}, \boldsymbol{x})\boldsymbol{x}$, where $A(\boldsymbol{y}, \boldsymbol{x})$ is the element displayed at row $\boldsymbol{y}$ and column $\boldsymbol{x}$ in the following table*:

	$\boldsymbol{a}$	$\boldsymbol{a}^{\uparrow}$	$\boldsymbol{b}$	$\boldsymbol{b}^{\uparrow}$	$\boldsymbol{c}$	$\boldsymbol{c}^{\uparrow}$
$\boldsymbol{a}$	I	$I^{\uparrow}$	P	$P^{\rightarrow}$	$P^{\vee}$	$P^{\uparrow}$
$\boldsymbol{a}^{\uparrow}$	$I^{\uparrow}$	I	$P^{\uparrow}$	$P^{\vee}$	$P^{\rightarrow}$	P
$\boldsymbol{b}$	$P^{\vee}$	$P^{\uparrow}$	I	$I^{\uparrow}$	P	$P^{\rightarrow}$
$\boldsymbol{b}^{\uparrow}$	$P^{\rightarrow}$	P	$I^{\uparrow}$	I	$P^{\uparrow}$	$P^{\vee}$
$\boldsymbol{c}$	P	$P^{\rightarrow}$	$P^{\vee}$	$P^{\uparrow}$	I	$I^{\uparrow}$
$\boldsymbol{c}^{\uparrow}$	$P^{\uparrow}$	$P^{\vee}$	$P^{\rightarrow}$	P	$I^{\uparrow}$	I

(14)

Proof. The relationships involving I and $I^{\uparrow}$ are trivial, and those involving P follow from Lemma 3.

- Thus we already know from (14) that $\boldsymbol{c} = P\boldsymbol{a}$, implying $\boldsymbol{c}^{\uparrow} \overset{(2l)}{=} I^{\uparrow}P\boldsymbol{a} \overset{(2e)}{=} P^{\uparrow}\boldsymbol{a}$ (see Lemma 1). This gives the $P^{\uparrow}$-entry at column $\boldsymbol{a}$ and row $\boldsymbol{c}^{\uparrow}$ in the table above. All

other $P^{\uparrow}$-entries follow from the symbolic substitutions induced by the invariance of the *BDP*-nature under the D_3^G-operations.

- Now $\boldsymbol{c}^{\uparrow} = P^{\uparrow}\boldsymbol{a} = P^{\uparrow}I^{\uparrow}\boldsymbol{a}^{\uparrow} \overset{(2i)}{=} P^{\uparrow}I^{\rightarrow}\boldsymbol{a}^{\uparrow} \overset{(2f)}{=} (P^{\uparrow})^{\rightarrow}\boldsymbol{a}^{\uparrow} \overset{(1)}{=} P^{\vee}\boldsymbol{a}^{\uparrow}$. This gives one $P^{\vee}$-entry in the table. The others are obtained by the allowed symbolic substitutions.
- So we find $\boldsymbol{b} = P^{\vee}\boldsymbol{a}$, implying $\boldsymbol{b}^{\uparrow} = I^{\uparrow}P^{\vee}\boldsymbol{a} \overset{(2e)}{=} (P^{\vee})^{\uparrow}\boldsymbol{a} \overset{(1)}{=} P^{\rightarrow}\boldsymbol{a}$. This initiates the $P^{\rightarrow}$-entries in the table. □

Lemma 4. *For all* $\boldsymbol{x},\boldsymbol{y},\boldsymbol{z} \in \mathscr{T} = \{\boldsymbol{a},\boldsymbol{a}^{\uparrow},\boldsymbol{b},\boldsymbol{b}^{\uparrow},\boldsymbol{c},\boldsymbol{c}^{\uparrow}\}$, *the following transitivity property holds between the elements of table* (14):

$$A(\boldsymbol{y},\boldsymbol{x}) = A(\boldsymbol{y},\boldsymbol{z})A(\boldsymbol{z},\boldsymbol{x}). \tag{15}$$

Proof. By definition, $\boldsymbol{y} = A(\boldsymbol{y},\boldsymbol{z})\boldsymbol{z} = A(\boldsymbol{y},\boldsymbol{z})A(\boldsymbol{z},\boldsymbol{x})\boldsymbol{x}$, and also $\boldsymbol{y} = A(\boldsymbol{y},\boldsymbol{x})\boldsymbol{x}$, implying that

$$[A(\boldsymbol{y},\boldsymbol{z})A(\boldsymbol{z},\boldsymbol{x}) - A(\boldsymbol{y},\boldsymbol{x})]\boldsymbol{x} = 0 \quad \text{for all } \boldsymbol{x},\boldsymbol{y},\boldsymbol{z} \in \mathscr{T}.$$

This expression must hold for any *value* of the vector $\boldsymbol{x}$, and this requires (15) to be true. □

We are now able to derive some remarkable properties concerning products of the $\langle 0,\vee,\uparrow,\rightarrow\rangle$-transforms of the Pascal matrix.

3.2. Product properties of the Pascal matrix transforms $P, P^{\uparrow}, P^{\rightarrow}, P^{\vee}$

Property 2. $D_3^{P_R} \overset{\text{def}}{=} \langle I, I^{\uparrow}, P, P^{\rightarrow}, P^{\uparrow}, P^{\vee}; \times_{\text{mod }2}\rangle$, (*all matrices in this set having the same arbitrary size*), *with* $\times_{\text{mod }2}$ *denoting the ordinary matrix product modulo 2, is a dihedral* D_3*-group with identity* I. *Its Cayley table is*

$\times_{\text{mod }2}$	I	$I^{\uparrow}$	P	$P^{\rightarrow}$	$P^{\uparrow}$	$P^{\vee}$
I	I	$I^{\uparrow}$	P	$P^{\rightarrow}$	$P^{\uparrow}$	$P^{\vee}$
$I^{\uparrow}$	$I^{\uparrow}$	I	$P^{\uparrow}$	$P^{\vee}$	P	$P^{\rightarrow}$
P	P	$P^{\rightarrow}$	$P^{\vee}$	$P^{\uparrow}$	$I^{\uparrow}$	I
$P^{\rightarrow}$	$P^{\rightarrow}$	P	$I^{\uparrow}$	I	$P^{\vee}$	$P^{\uparrow}$
$P^{\uparrow}$	$P^{\uparrow}$	$P^{\vee}$	$P^{\rightarrow}$	P	I	$I^{\uparrow}$
$P^{\vee}$	$P^{\vee}$	$P^{\uparrow}$	I	$I^{\uparrow}$	$P^{\rightarrow}$	P

(16)

(*Convention*: *the matrix product* XY *is found at the crossing of row* X *and column* Y)

Proof. Apply Lemma 4 with $\boldsymbol{z} = \boldsymbol{a}$ to obtain $A(\boldsymbol{y},\boldsymbol{x}) = A(\boldsymbol{y},\boldsymbol{a})A(\boldsymbol{a},\boldsymbol{x})$. Referring to table (14), this particular transitivity property can be interpreted as follows: every element in row $\boldsymbol{y}$ can be obtained by premultiplying the corresponding element in the first row of the table with the first element in row $\boldsymbol{y}$. For example, applying this to the elements of row $\boldsymbol{b}^{\uparrow}$ in (14) produces row $P^{\rightarrow}$ in (16): $P^{\rightarrow} = P^{\rightarrow}I$, $P = P^{\rightarrow}I^{\uparrow}$, $I^{\uparrow} =$

$P^{\rightarrow}P$, $I=P^{\rightarrow}P^{\rightarrow}$, $P^{\uparrow}=P^{\rightarrow}P^{\vee}$, $P^{\vee}=P^{\rightarrow}P^{\uparrow}$. Another interpretation is that every element in column $\boldsymbol{x}$ of table (14) can be obtained by postmultiplying the corresponding element in the first column of the table with the first element in column $\boldsymbol{x}$. Both interpretations establish the multiplication table (16). Inspection shows that this table is isomorphic to the D_3^G-table (7) under the bijective mapping

$$\mathscr{G}: D_3^G \to D_3^{P_R} : R_{0^\circ} \mapsto I, M_1 \mapsto I^{\uparrow}, R_{240^\circ} \mapsto P, R_{120^\circ} \mapsto P^{\vee}, \\ M_3 \mapsto P^{\uparrow}, M_2 \mapsto P^{\rightarrow}. \quad \square \tag{17}$$

Remark 2. The superscript P_R in the group notation $D_3^{P_R}$ introduced in the previous Property 2 refers to the appearance of the $R=\langle 0, \vee, \uparrow, \rightarrow\rangle$-transforms of the Pascal matrix P (recall the comment following Lemma 1).

Corollary 1. *Whatever the size of the Pascal matrix, the following remarkable product properties always hold*:

$$P^3 = (P^{\vee})^3 = (P^{\uparrow})^2 = (P^{\rightarrow})^2 = I, \tag{18a}$$

$$P^2 = P^{\vee}, \ (P^{\vee})^2 = P. \tag{18b}$$

Remark 3. The isomorphism of $D_3^{P_R}$ with D_3^G under mapping (17) can be given a nice "analytic-geometric" interpretation, in the sense that the result of a geometric operation can also be obtained by evaluation of an analytic expression. This will be explained using Fig. 6, which is basically the same as Fig. 5, but displays only the *top-edge sequences* of the BDPs in $\mathscr{U}=\{A,B,C,D,E,F\}$ shown in Fig. 5. This set of top-edge sequences is $\mathscr{T}^*=\{\boldsymbol{a},\boldsymbol{a}^{\uparrow},\boldsymbol{b},\boldsymbol{b}^{\uparrow},\boldsymbol{c},\boldsymbol{c}^{\uparrow}\}$ (we use $\mathscr{T}^*$ in order to stress the fact that its elements must appear as top-edge sequences, see further). First observe that any geometric operation from D_3^G maps a given top-edge sequence into another top-edge sequence. This is a result of the group action $\phi_{G,\mathscr{U}}: D_3^G \times \mathscr{U} \to \mathscr{U}$ represented in Fig. 5, while restricting the BDPs in $\mathscr{U}$ to their corresponding top-edge sequences , so that we actually consider the action

$$\phi_{G,\mathscr{T}^*} : D_3^G \times \mathscr{T}^* \to \mathscr{T}^*, \tag{19}$$

represented in Fig. 6. For example, under this action, M_2 sends $\boldsymbol{a}$ into $\boldsymbol{b}^{\uparrow}$ (as top-edge sequences; this is no longer true when $\boldsymbol{a}$ is the left-side sequence of BDP C in Fig. 5: then M_2 sends this left-side edge $\boldsymbol{a}$ into $\boldsymbol{a}^{\uparrow}$. This is the reason why it is important to distinguish between $\mathscr{T}^*$ and $\mathscr{T}$).

On the other hand, tables (14) and (16) allow us to verify that, for any W_1, $W_2 \in D_3^{P_R}$ and for any $\boldsymbol{v} \in \mathscr{T}$, it holds that $(W_2W_1)\boldsymbol{v} = W_2(W_1\boldsymbol{v})$ (usual matrix product in $\mathbb{F}_2$). As a consequence, the mapping

$$\phi_{P_R,\mathscr{T}} : D_3^{P_R} \times \mathscr{T} \to \mathscr{T} : (W, \boldsymbol{v}) \mapsto W\boldsymbol{v} \tag{20}$$

defines a group action of $D_3^{P_R}$ on $\mathscr{T}$. As $\mathscr{T}$ is the set of edge-sequences $\{\boldsymbol{a},\boldsymbol{a}^{\uparrow},\boldsymbol{b},\boldsymbol{b}^{\uparrow},\boldsymbol{c},\boldsymbol{c}^{\uparrow}\}$ in the mutual geometric relationship shown in Fig. 5, and as a consequence also in their

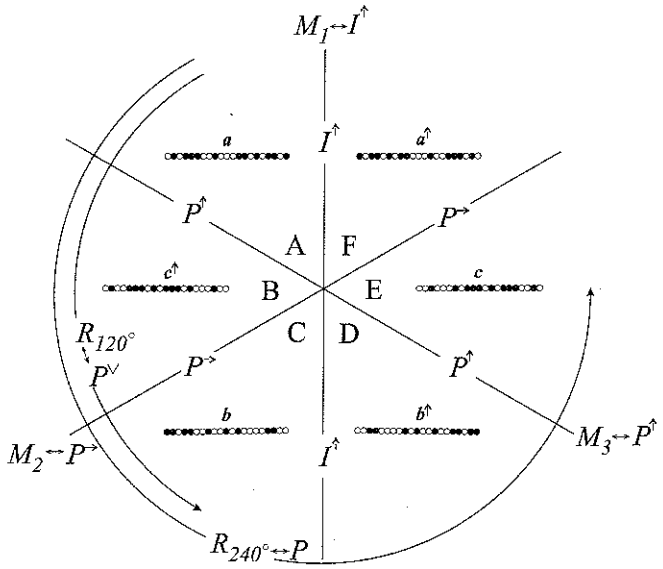


Fig. 6. "Analytic-geometric" interpretation of the isomorphism $\mathscr{G}$ that maps the group $D_3^G = \langle R_{0^\circ}, M_1, R_{240^\circ}, M_3, M_2, R_{120^\circ}; \circ \rangle$ into the group $D_3^{P_R} = \langle I, I^{\uparrow}, P, P^{\uparrow}, P^{\rightarrow}, P^{\vee}; \times_{\mathrm{mod}\,2} \rangle$ (mapping elementwise in the given order). This isomorphism induces an isomorphism between the "geometric" action of D_3^G on $\mathscr{T}^* = \{\boldsymbol{a}, \boldsymbol{a}^{\uparrow}, \boldsymbol{b}, \boldsymbol{b}^{\uparrow}, \boldsymbol{c}, \boldsymbol{c}^{\uparrow}\}$ and the "analytic" action of $D_3^{P_R}$ on $\mathscr{T}^*$. With $\boldsymbol{v} \in \mathscr{T}^*$, g and $h \in D_3^G$, $\boldsymbol{v}$ maps into $h \circ g(\boldsymbol{v})$ under the geometric operation $h \circ g$, and $h \circ g(\boldsymbol{v}) = \mathscr{G}(h)\mathscr{G}(g)\boldsymbol{v}$.

relationship as top-edge sequences, action (20) also works on the top-edge sequences displayed in Fig. 6, or

$$\phi_{P_R,\mathscr{T}^*} : D_3^{P_R} \times \mathscr{T}^* \to \mathscr{T}^* : (W, \boldsymbol{v}) \mapsto W\boldsymbol{v} \tag{21}$$

defines an action from $D_3^{P_R}$ on $\mathscr{T}^*$. As D_3^G and $D_3^{P_R}$ are isomorphic, it follows that both the "geometric" action $\phi_{G,\mathscr{T}^*}$ and the "analytic" action $\phi_{P_R,\mathscr{T}^*}$ are isomorphic [14], and that we can write, for all $g, h \in D_3^G$ and all $v \in \mathscr{T}^*$:

$$g(\boldsymbol{v}) = \mathscr{G}(g)\boldsymbol{v}, \tag{22}$$

$$(h \circ g)(\boldsymbol{v}) = \mathscr{G}(h \circ g)\boldsymbol{v} = \mathscr{G}(h)\mathscr{G}(g)\boldsymbol{v}. \tag{23}$$

These equations explain why we have also written the matrix $\mathscr{G}(g)$ next to each g-operation in Fig. 6. For example, from Fig. 6, one can read that $\boldsymbol{a}^{\uparrow} = M_3(\boldsymbol{b}) = P^{\uparrow}\boldsymbol{b}$. Also: $\boldsymbol{a}^{\uparrow} = M_3(\boldsymbol{b}) \overset{(7)}{=} M_2 \circ R_{120^\circ}(\boldsymbol{b}) = P^{\rightarrow}P^{\vee}\boldsymbol{b}$ (which corresponds to $P^{\rightarrow}P^{\vee} = P^{\uparrow}$ in the Cayley-table (16)).

4. BDPs with particular symmetries

We already know that BDPs remain BDPs under the D_3^G operations. Are there BDPs which remain, *as a geometric pattern* (and not only in nature), invariant under some of these operations? How to find these symmetric BDPs? How many of them are there?

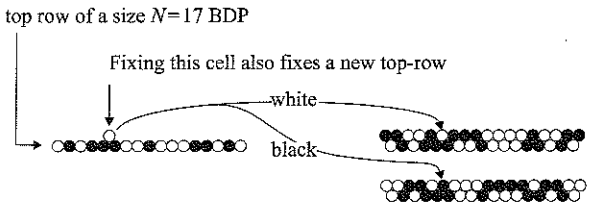


Fig. 7. Adding a new row on top of a BDP.

These are the questions that will be dealt with in this section. But first, we present a procedure for "growing" BDPs.

4.1. Rowwise extension of a BDP

A BDP of size N with top row $\boldsymbol{a}_N$ can be extended to a BDF of size $N+1$, by adding a top row $\boldsymbol{a}_{N+1}$. Such $\boldsymbol{a}_{N+1}$ is completely determined by fixing one of its elements, as all other a_{N+1}-values can be obtained by using the local matching rule, as illustrated in Fig. 7. Observe that the two possible extension sequences are complementary, i.e., a white cell in one sequence corresponds to a black one in the other sequence and vice versa. This procedure can of course be repeated to extend a given BDP to a BDP of any larger size. It can also be applied for extensions on either the left or the right side of the BDP. For any row thus added, there are two possible extensions.

4.2. BDPs with palindromic (S_2^G) symmetry

$S_2^G = \langle R_{0^\circ}, M; \circ \rangle$ denotes the *symmetric group* [10,12] of geometric operations which leave an isosceles triangle invariant: rotation by 0° (the identity operation), and M: reflection about the median that bisects the angle formed by the equal edges. The adjective "palindromic" is inspired by the following property.

Property 3. (a) *A BDP with a reflection-symmetric top-edge sequence (or palindrome), i.e., $\boldsymbol{a} = \boldsymbol{a}^\uparrow$, is overall symmetric under reflection about the vertical median, and vice versa.*

(b) $\boldsymbol{c} = \boldsymbol{b}^\uparrow \Leftrightarrow \boldsymbol{a} = \boldsymbol{a}^\uparrow$.

Proof. Assumption (a) is a consequence of the obvious fact that difference sequences of palindrome sequences are palindromes themselves.

(b) $\Leftarrow$-part: Follows from (a).

$\Rightarrow$-part: $\boldsymbol{c} = \boldsymbol{b}^\uparrow$ together with $\boldsymbol{c} \overset{(14)}{=} P\boldsymbol{a}$ and $\boldsymbol{b}^\uparrow \overset{(14)}{=} P\boldsymbol{a}^\uparrow$ implies that $P(\boldsymbol{a} + \boldsymbol{a}^\uparrow) = 0$. Invertibility of P (see Lemma 2) then implies $\boldsymbol{a} = \boldsymbol{a}^\uparrow$. □

Definition 3. a BDP that is symmetric about its vertical median is *a palindrome-symmetric* BDP (or has palindromic symmetry).

Property 4. *The number of different N-sized palindrome-symmetric BDPs is* $2^{\lceil N/2 \rceil}$.

Proof. Is a trivial consequence of the fact that a BDP is completely determined by its top-edge sequence. The condition $\boldsymbol{a} = \boldsymbol{a}^{\uparrow}$ allows that any $\lceil N/2 \rceil$ elements of $\boldsymbol{a}$, no two of which are located symmetric with respect to the median, can be attributed the value 0 or 1 (white or black) in an arbitrary way. Different ways of attributing 0/1-values to these cells produce different BDPs. □

Remark 4. Each cell that can be given an arbitrary value in the solution of a problem, represents a *degree of freedom* . The number of such cells will be called the *number of degrees of freedom F*.

For palindromic BDPs, this number is

$$F_P = \left\lceil \frac{N}{2} \right\rceil . \tag{24}$$

Definition 4. A *median-centered* sub-BDP of a given BDP is any BDP that is contained in the original BDP and has the same median.

Property 5. (a) *Any median-centered sub-BDP of a palindrome-symmetric BDP is also palindrome-symmetric.*

(b) *All cells of a palindrome-symmetric BDP that are located on the median must be white (have value 0), except the one on the top row, which may be either black or white. In case it is black, the BDP cannot be expanded by top-row extension under conservation of the palindromic symmetry.*

Proof. Assumption (a) is trivial.

(b) Consider a palindrome-symmetric BDP of size N, with top-row sequence $\boldsymbol{a}_N = \boldsymbol{a}_N^{\uparrow}$. Two possibilities have to be taken into account when we want to expand the BDP — under conservation of the palindromic symmetry — by adding a new top-row sequence $\boldsymbol{a}_{N+1}$ as explained under Section 4.1 above.

If $N = even$, two mutually complementary palindrome sequences $\boldsymbol{a}_{N+1}$ are possible. This is illustrated in Fig. 8(a) when, for example, $\boldsymbol{a}_{N+1}(N/2)$ is getting fixed.

If $N = odd$, and the median element $\boldsymbol{a}_N(\lceil N/2 \rceil) = 0$ (white cell), then again two complementary palindrome extensions $\boldsymbol{a}_{N+1}$ are possible. However, no extension is possible when $\boldsymbol{a}_N(\lceil N/2 \rceil) = 1$, because the local matching rule would imply that the two median-adjacent cells of the extension row $\boldsymbol{a}_{N+1}$ must be different. Actually, both the first and second half of $\boldsymbol{a}_{N+1}$ would be reverse complementary [see Fig. 8(b)]. This breaks down the required palindrome symmetry. Thus, if a palindrome-symmetric BDP has a black median top-row cell, it cannot be be expanded at the top-edge. That is also the reason why all internal median cells have to be white: all these cells can be considered as the median cell of the top row of a sub-BDP from which the original BDP can be constructed by proper top-row extension. But this cell being black would make such an extension impossible. As the extension is possible however, we conclude — by contradiction — that all internal median cells have to be white. □

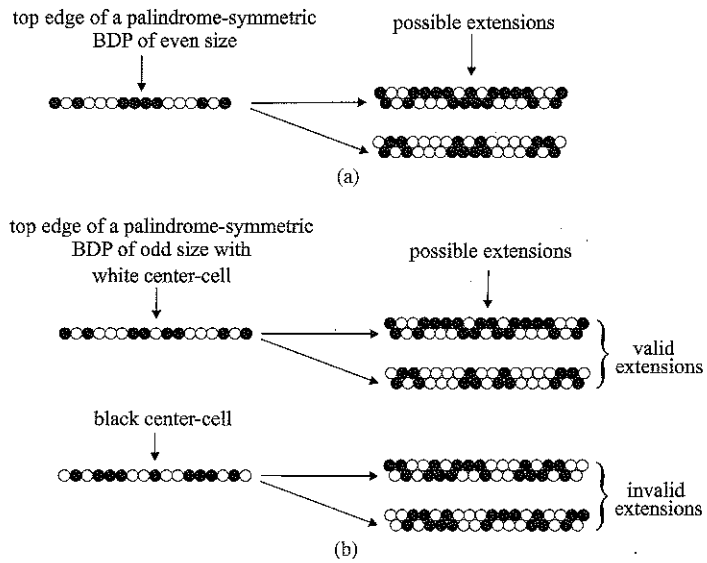


Fig. 8. Top-row expansion of: (a) a palindrome-symmetric BDP of even size, and (b) of odd size.

4.3. BDPs with rotational ($\langle R^{\circ}_{120}\rangle$) symmetry

$\langle R^{\circ}_{120}\rangle$ refers to the cyclic group of the geometric rotation-operations R_{0° (the identity), $R_{120^\circ}, R_{240^\circ}$. This section deals with *rotationally symmetric* BDPs, i.e., BDPs that, as patterns, are invariant under the $\langle R^{\circ}_{120}\rangle$-operations. It is clear that a necessary and sufficient condition for this is that $\boldsymbol{a} = \boldsymbol{b} = \boldsymbol{c}$ (because the BDP of a sequence is uniquely determined).

Property 6. (a) $\boldsymbol{a} = \boldsymbol{b} \Leftrightarrow \boldsymbol{a} = \boldsymbol{b} = \boldsymbol{c}$, *i.e. BDPs that satisfy the first condition exhibit rotational symmetry.*

(b) $\boldsymbol{a}$ *is a top-edge sequence of a rotationally symmetric BDP if and only if it satisfies the equation*

$$[I + P]\boldsymbol{a} = 0. \tag{25}$$

Proof. As $\boldsymbol{b} \overset{(14)}{=} P^{\vee}\boldsymbol{a}$ and $\boldsymbol{c} \overset{(14)}{=} P^{\vee}\boldsymbol{b}$, the condition $\boldsymbol{a} = \boldsymbol{b}$ implies that $\boldsymbol{c} = \boldsymbol{b}$. This proves (a). But then also $\boldsymbol{a} = P^{\vee}\boldsymbol{a}$ holds, or $[I + P^{\vee}]\boldsymbol{a} = 0$. Premultiplying both sides of this equation with the (invertible) Pascal matrix P produces (25). Conversely, if (25) holds, premultiply its both sides with the invertible $P^{\vee}$ to obtain $P^{\vee}\boldsymbol{a} = \boldsymbol{a}$, or $\boldsymbol{b} = \boldsymbol{a}$. According to (a), this implies rotational symmetry. □

The $\langle R_{120^\circ}\rangle$-symmetric BDPs of size N can be found by solving Eq. (25), for size N, with respect to the top edge sequence $\boldsymbol{a}_N$. This can be done by bringing the matrix $[I_N + P_N]$ in *row-reduced echelon form*. This produces solutions for $a(0), a(1), \ldots, a(N-1)$

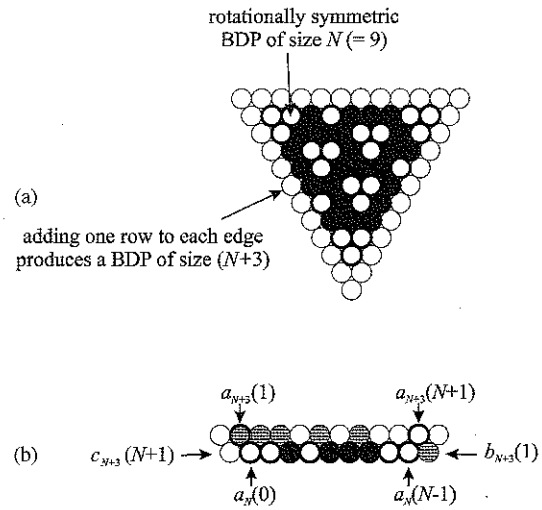


Fig. 9. Expanding a rotationally symmetric BDP of size N to size $(N+3)$ [see (a)] can be done by fixing a single cell in the expanding top row [see (b)].

in which there are F_R elements $a(f_1), a(f_2), \ldots, a(f_{F_R})$ that are free variables, and $(N - F_R)$ dependent variables. No particular rule has been found which determines the set of free variables as a function of N without actually generating the row echelon form. However, the number of free variables F_R, as function of N, is given by

Property 7. *The number of degrees of freedom $F_R(N)$ in the N-sized rotationally symmetric BDP construction is, for $N \geqslant 3$,*

$$F_R(N) = \left\lfloor \frac{N}{3} \right\rfloor + [(N \bmod 3) \bmod 2]. \tag{26}$$

Proof. Consider a rotationally symmetric BDP of size N, with $\boldsymbol{a}_N = \boldsymbol{b}_N = \boldsymbol{c}_N$. By adding an additional row of cells to each edge of this BDP, we obtain a BDP of size $N+3$ [see Fig. 9(a)]. We will show that the original BDP can be expanded, under preservation of the rotational symmetry ($\boldsymbol{a}_{N+3} = \boldsymbol{b}_{N+3} = \boldsymbol{c}_{N+3}$), in only two ways. Because of the rotational symmetry, we only have to consider the extension of the top-edge sequence $\boldsymbol{a}_N$ [see Fig. 9(b)].

Start with either a white or black cell $a_{N+3}(1)$ as top-left neighbouring cell of $a_N(0)$. Applying the local matching rule then fixes all cell-states to the right of $a_{N+3}(1)$, one by one, from left to right, until $a_{N+3}(N+1)$ is reached.

Invoking the symmetry conditions $c_{N+3}(N+1) = a_{N+3}(N+1)$ and $b_{N+3}(1) = a_{N+3}(1)$ then fixes $c_{N+3}(N+1)$ and $b_{N+3}(1)$. This determines the complete $(N+3)$-sized rotationally symmetric BDP. Remember that the whole expansion depends only on the arbitrary fixing of the $a_{N+3}(1)$-cell: thus only one degree of freedom appears in the transition from size N to size $N+3$ (notice that the expansion-sequences corresponding to the two possibilities are complementary). This explains why the number of

possible $(N+3)$-sized rotationally symmetric BDPs equals twice the number of N-sized rotationally symmetric BDPs. Or, in terms of the number of degrees of freedom

$$F_R(N+3) = F_R(N) + 1. \tag{27}$$

We only need the initial values $F_R(1), F_R(2), F_R(3)$ in order to solve this recursion. These values follow from solving (25) for $N = 1, 2, 3$ and yields

$$F_R(1) = 1, \quad F_R(2) = 0, \quad F_R(3) = 1.$$

Applying (27) produces a sequence $(F_R(N))_{N \geqslant 1}$ which is easily verified to correspond with (26) [check that (26) satisfies the initial conditions and the recursion (27)]. □

Remark 5. Thus, the number of solutions of (25), and also the number of rotationally symmetric BDPs equals 2^{F_R}. As (25) is a set of homogenous linear equations over $\mathbb{F}_2$, all its $\boldsymbol{a}$-solutions form a group G_{sol} under componentwise addition modulo 2. This group is isomorphic to the group G_f of the free variable configuration strings $[a(f_1)a(f_2)\ldots a(f_{F_R})]$ under componentwise addition modulo 2, and this group is in its turn isomorphic to the Abelian product group $(\mathbb{F}_2)^{F_R}$. As the local rule for producing the complete BDP from the top-edge sequence $\boldsymbol{a}$ is linear in $\mathbb{F}_2$, this group property for the free variable strings is also inherited by the corresponding BDPs under cellwise addition modulo 2. This group of BDPs will be represented by G_{BDP}. A "natural" minimal generator set for G_f (and the isomorphic set for the other groups G_{sol} and G_{BDP}), is the set of F_R free variable configurations $[a(f_1)a(f_2)\ldots a(f_{F_R})]$ in which only one of these free variables gets the value 1 and the others the value 0. Fig. 10 shows this generator set for $N = 21$, together with a few other solutions. Observe that some of the solutions show D_3^G-symmetry (Figs. 10(g),(k) and (l)).

Property 8. *In a rotationally symmetric BDP of size $N = 2^k + 1$, all vertex-cells are white*: $a(0) = b(0) = c(0) = 0$.

Proof. $\boldsymbol{a}_N$ is a solution of $[I_N + P_N]\boldsymbol{a}_N = 0$ [Eq. (25)]. When $N = 2^k + 1$, the top row of P_N (consisting of the coefficients $\binom{2^k}{m} \bmod 2, m = 0, \ldots, 2^k$) is always of the form $100\ldots01$, while the bottom row is always $100\ldots00$. It follows that $[I_N + P_N]$ has top row $000\ldots01$, and bottom row $100\ldots01$. This corresponds to the equations $a_N(N-1)=0$ and $a_N(0)+a_N(N-1)=0$. Invoking the rotational symmetry, this results in the property as stated. □

Remark 6. If $N \neq 2^k + 1$, the symmetry requires that the vertex cells are all the same, but they may be either black or white.

4.4. BDPs with dihedral (D_3^G) symmetry

Here we discuss the conditions for full dihedral symmetry of a BDP, requiring that it is invariant under any of the D_3^G-operations. It is clear that it is necessary and sufficient that $\boldsymbol{a} = \boldsymbol{a}^{\uparrow} = \boldsymbol{b} = \boldsymbol{b}^{\uparrow} = \boldsymbol{c} = \boldsymbol{c}^{\uparrow}$.

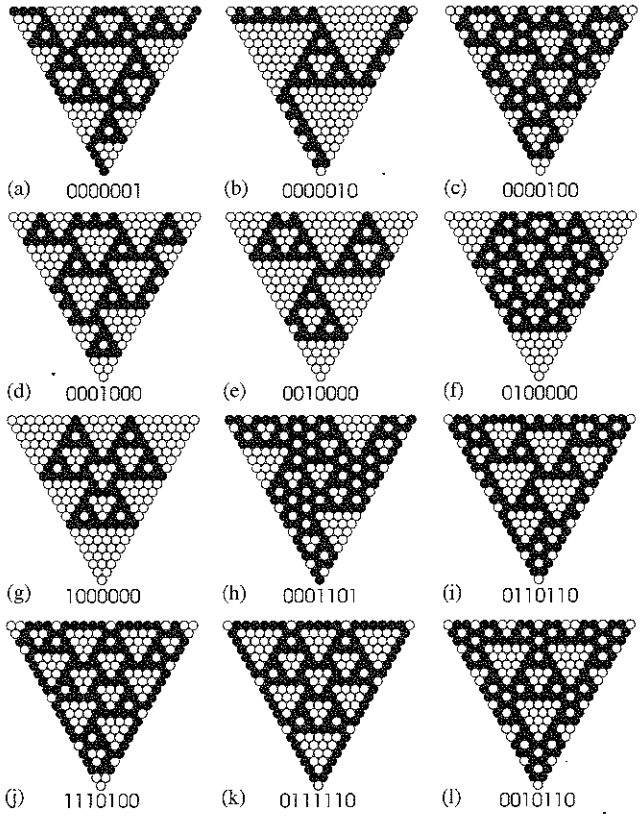


Fig. 10. (a)–(g) The "natural" generator set -consisting of 7 solutions- for the rotationally symmetric BDPs of size $N = 21$. The complete solution set can be obtained by cellwise addition modulo 2 of solutions in this generator set. The binary strings represent the values of the corresponding free-variable string $a(13)a(14)a(15)a(17)a(18)a(19)a(20)$. (h)–(l) Five additional solutions. As the free-variable code of (h) is the elementwise sum modulo 2 of the free-variable codes of (a), (c), (d), pattern (h) is the cellwise sum modulo 2 of patterns (a), (c), (d).

Property 9. (a) $\boldsymbol{a} = \boldsymbol{a}^{\uparrow} = \boldsymbol{b}$ *implies dihedral symmetry.*

(b) *Let* $\boldsymbol{a}_{\lceil N/2 \rceil}$ *be the vector whose elements are the* $\lceil N/2 \rceil$ *first elements of the top row edge* $\boldsymbol{a}_N$ *of a dihedrally symmetric BDP of size N, then* $\boldsymbol{a}_{\lceil N/2 \rceil}$ *satisfies the equation*

$$[S_1 + \overrightarrow{S_2}]\boldsymbol{a}_{\lceil N/2 \rceil} = 0, \tag{28}$$

where S_1 *and* S_2 *are obtained from the* $[S_1|S_2']$ *partitioning of the matrix* $[I + P]$ *into two blocks of* $\lceil N/2 \rceil$ *and* $N - \lceil N/2 \rceil$ *columns respectively, and where* $S_2 = S_2'$ *if N is even, and* $S_2 = [0|S_2']$ *if N is odd (i.e.,* S_2 *equals* S_2' *augmented with one leftmost column of* 0*s). The other elements of* $\boldsymbol{a}_N$ *follow from the reflective symmetry condition*

$$a(N - k - 1) = a(k) \quad for\ k \leqslant \lceil N/2 \rceil. \tag{29}$$

Conversely, any solution of Eqs. (28)–(29) *produces a top-edge sequence of a dihedrally symmetric BDP.*

Proof. (a) Follows from the fact that $\boldsymbol{a} = \boldsymbol{b}$ implies rotational symmetry (Property 6), while $\boldsymbol{a} = \boldsymbol{a}^{\uparrow}$ implies reflective symmetry about the median M_1, which under the rotational symmetry also produces reflection symmetry about the two other medians.

(b) Eq. (28) is a straightforward reduction of Eq. (25): $[I + P]\boldsymbol{a} = 0$ (equivalent to $\boldsymbol{a} = \boldsymbol{b}$), using the condition $\boldsymbol{a} = \boldsymbol{a}^{\uparrow}$ (29). The converse statement in (b) follows from reversing the argumentation showing that (28) is equivalent to $[I+P]\boldsymbol{a}=0$, with $\boldsymbol{a}=\boldsymbol{a}^{\uparrow}$. □

Property 10. *The condition* $\boldsymbol{a}=\boldsymbol{a}^{\uparrow}$ & $\boldsymbol{b}=\boldsymbol{b}^{\uparrow}$ *implies* $\boldsymbol{a}=\boldsymbol{b}$, *and thus dihedral symmetry of the BDP.*

Proof. We prove the equivalency of this condition with $\boldsymbol{a} = \boldsymbol{a}^{\uparrow} = \boldsymbol{b}$ for the nontrivial part.

We have

$$\boldsymbol{b} \overset{(14)}{=} P^{\vee}\boldsymbol{a} \overset{\text{premises}}{=} P^{\vee}\boldsymbol{a}^{\uparrow} \overset{(14)}{=} \boldsymbol{c}^{\uparrow},$$

$$\boldsymbol{b}^{\uparrow} \overset{(14)}{=} P^{\rightarrow}\boldsymbol{a} \overset{\text{premises}}{=} P^{\rightarrow}\boldsymbol{a}^{\uparrow} \overset{(14)}{=} \boldsymbol{c}.$$

As $\boldsymbol{b}=\boldsymbol{b}^{\uparrow}$, this implies $\boldsymbol{c}=\boldsymbol{c}^{\uparrow}$, and thus $\boldsymbol{b} \overset{(14)}{=} P\boldsymbol{c}$ implies $\boldsymbol{b}^{\uparrow} = P\boldsymbol{c}^{\uparrow}$. Comparing this last expression with $\boldsymbol{a}^{\uparrow} \overset{(14)}{=} P\boldsymbol{c}^{\uparrow}$ implies $\boldsymbol{b} = \boldsymbol{a}$. Thus, we conclude that the premises lead to $\boldsymbol{a} = \boldsymbol{a}^{\uparrow} = \boldsymbol{b}$, and, through Property 9, to dihedral symmetry. □

Remark 7. Because all edges of the BDP can be treated in the same way, the two previous properties remain valid under the cyclic substitution $\boldsymbol{a} \mapsto \boldsymbol{b} \mapsto \boldsymbol{c} \mapsto \boldsymbol{a}$. Property 10 implies that a BDP cannot have two different palindromic edges. A BDP has either only one palindromic edge, implying *strict* palindromic symmetry, or three identical palindromic edges, implying dihedral symmetry.

Remark 8. As D_3^G-symmetric BDPs have palindromic as well as rotational symmetry, Property 5 for palindrome-symmetric BDPs now applies to all medians: all cells located on any of the medians must be white, except those on the edges (for odd-sized BDPs). In case the edge-median cells are black, the BDP cannot be extended under preservation of the D_3^G-symmetry.

Property 11. *The number of degrees of freedom* $F_D(N)$ *in the* N*-sized* D_3^G*-symmetric BDP construction* [*or the number of free variables in the solution of Eq.* (28)], *is given by*

$$F_D(N) = \left\lfloor \frac{N+3}{6} \right\rfloor + \delta_{1,(N \bmod 6)}, \tag{30}$$

where $\delta_{1,m} = 1$ *if* $m = 1$, *else* $\delta_{1,m} = 0$.

Proof. We will count the possibilities in which a dihedrally symmetric BDP of size N can be expanded into one of size $(N + 3)$, by applying the row-extension procedure, just like in Fig. 9. Start by considering its palindromic top-row sequence vector $\boldsymbol{a}_N$:

- When $N=$ *even*, there are two possible extensions, corresponding to the selections $a_{N+3}(N/2)=0$ or 1, respectively. When $a_{N+3}(N/2)=1$, is selected, the expansion thus obtained is a *terminal* one, because a further expansion would destroy the palindrome-symmetry, and hence also the dihedral symmetry.
- When $N=$ *odd* and (a): $a_N(\lfloor N/2\rfloor)=1$, the BDP is terminal, and cannot be expanded, and (b): $a_N(\lfloor N/2\rfloor)=0$, there are again two *nonterminal* BDPs of size $(N+3)$, corresponding to the two possible values that can be given to $a_{N+3}(1)$ (as in the proof of Property 7).

Denoting by $\mathscr{D}(N)$ the set of dihedrally symmetric BDPs of size N, and by $\mathscr{D}_{\mathrm{NT}}(N)$ and $\mathscr{D}_{\mathrm{T}}(N)$ the sets of nonterminal and terminal dihedrally symmetric BDPs, respectively, the above findings can be summarized by the following recursions for the corresponding cardinalities:

For $N\geqslant 0$:

$$|\mathscr{D}_{\mathrm{NT}}(N+3)|=|\mathscr{D}_{\mathrm{NT}}(N)|, \tag{31a}$$

$$|\mathscr{D}_{\mathrm{T}}(N+3)|=|\mathscr{D}_{\mathrm{NT}}(N)| \quad \text{when } N \text{ is even } ((N+3) \text{ is odd}), \tag{31b}$$

$$|\mathscr{D}_{\mathrm{NT}}(N+3)|=2|\mathscr{D}_{\mathrm{NT}}(N)|, \tag{31c}$$

$$|\mathscr{D}_{\mathrm{T}}(N+3)|=0 \quad \text{when } N=\text{is odd } ((N+3) \text{ is even}) \tag{31d}$$

and

$$|\mathscr{D}(N)|=|\mathscr{D}_{\mathrm{NT}}(N)|+|\mathscr{D}_{\mathrm{T}}(N)|. \tag{32}$$

(It will be convenient to consider $\mathscr{D}(0)$ as containing the "empty" BDP, which is nonterminal. Thus $|\mathscr{D}_{\mathrm{NT}}(0)|=1$, $\mathscr{D}_{\mathrm{T}}(0)=0$ and $|\mathscr{D}(0)|=1$, and then (31a), (31b) and (32) do indeed hold for $N=0$.) Using the above expressions to calculate $|\mathscr{D}(N+6)|$ when $(N+6)$ is even (and thus $(N+3)$ is odd, and N is even), and $|\mathscr{D}(N+3)|$ when $(N+3)$ is odd (and thus N is even), produces the following recursions in $|\mathscr{D}(N)|$:

When N $(\geqslant 0)$ is *even*:

$$|\mathscr{D}(N+6)|=2|\mathscr{D}(N)|, \tag{33a}$$

$$|\mathscr{D}(N+3)|=2|\mathscr{D}(N)|. \tag{33b}$$

Now, when N is *even* $(N\geqslant 0)$, both $(N+9)$ and $(N+3)$ are odd, and we have

$$|\mathscr{D}(N+9)| \overset{(33b)}{=} 2|\mathscr{D}(N+6)| \overset{(33a)}{=} 2\times 2|\mathscr{D}(N)| \overset{(33b)}{=} 2|\mathscr{D}(N+3)|,$$

which is, by substituting N for $N+3$, equivalent to

$$|\mathscr{D}(N+6)|=2|\mathscr{D}(N)| \quad \text{for } N \textit{ odd} \text{ and } N\geqslant 3. \tag{34}$$

From (33b), we find that $|\mathscr{D}(7)|=2|\mathscr{D}(4)|$. Solving Eq. (28) for $N=4$ and 1, or direct construction of the dihedrally symmetric BDPs of these sizes, show that $|\mathscr{D}(4)|=$

$|\mathscr{D}(1)|(=2)$. This allows us to write $|\mathscr{D}(7)| = 2|\mathscr{D}(1)|$, meaning that (34) also holds for $N = 1$. This fact, and joining (33a) and (34), allows us to state that

$$|\mathscr{D}(N+6)| = 2|\mathscr{D}(N)| \quad \text{for all } N \geqslant 0. \tag{35}$$

Expressed in terms of the number of degrees of freedom $F_D(N)$ $(=\log_2|\mathscr{D}(N)|)$, this yields the recursion

$$F_D(N+6) = F_D(N) + 1. \tag{36}$$

This recursion can be solved from the initial conditions that can be obtained either from solving Eq. (28) or from direct construction of the corresponding BDPs:

$$F_D(1) = 1, \quad F_D(2) = 0, \quad F_D(3) = 1, \quad F_D(4) = 1, \quad F_D(5) = 1, \quad F_D(6) = 1. \tag{37}$$

Eq. (30) satisfies both (36) and (37), and so it is the closed form solution of recursion (36). □

Corollary 2.

$$F_D(N) = \left\lceil \frac{F_R(N)}{2} \right\rceil. \tag{38}$$

Proof. Observe that $F_D(N)$ as given by (38) satisfies (36), (37). □

Remark 5, concerning the group structure of the solutions for the rotationally symmetric case, can actually be extended to the D_3^G-case: all solutions of (28), (29), all free-variable configurations of these equations, and all related BDPs form Abelian groups under elementwise addition modulo 2 which are all isomorphic to $(\mathbb{F}_2)^{F_D(N)}$. Clearly, these groups form subgroups of the corresponding groups in the palindrome-symmetric and rotationally symmetric cases. A generator for the BDP-solutions group is formed by F_D independent solutions. Fig. 11 shows the 15 nontrivial dihedrally symmetric BDPs of size 21. As all these BDPs are also palindromic, those with a black cell in the middle of the edges (a,c,e,g,i,k,m,o) cannot be extended [Property 5(b)] and cannot occur as center-BDPs of dihedrally symmetric BDPs of larger size.

4.5. Congruent and incongruent BDPs

Applying one of the D_3^G-operations on a given BDP transforms it into another BDP which may or may not be the same as the original one. For example, a rotationally symmetric BDP which is not dihedrally symmetric (we call this a *strictly* rotationally symmetric BDP) produces, after reflection about a median, a rotationally symmetric BDP which differs from the original one (for example, this is so for all BDPs in Fig. 10, except (g), (k), (l)). However, if we consider a BDP as some physical object (e.g., as some kind of flat "molecule" consisting of black and white "atoms") that can be picked up and rotated by 180° around that median, these two different BDP-configurations

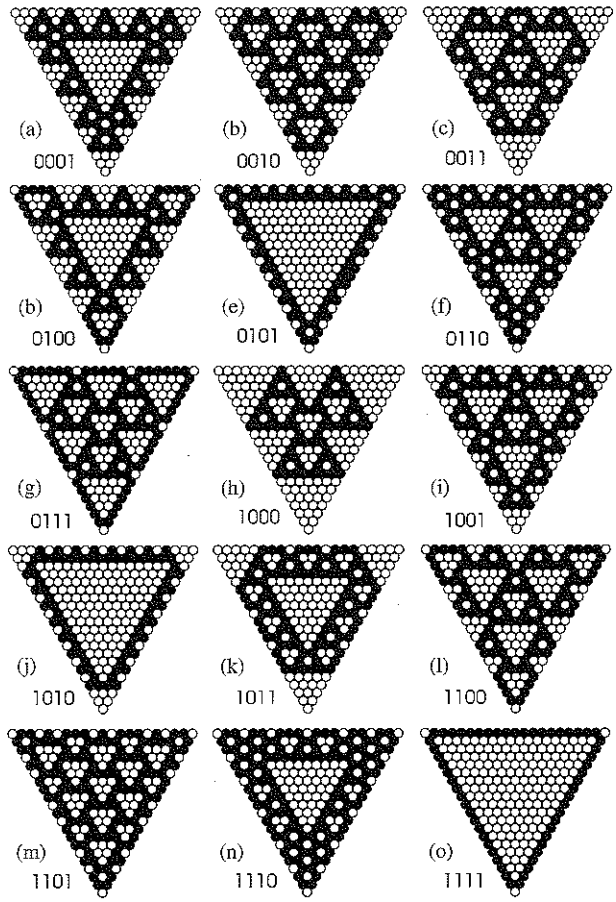


Fig. 11. The 15 nontrivial D_3^G-symmetric BDPs of size 21. The binary strings represent the code for the free-variable string $a(7)a(8)a(9)a(10)$ in the solution of Eqs. (28), (29). Any set of four of these solutions whose codes are linearly independent under elementwise addition modulo 2 forms a generator set: all other patterns can be obtained from cellwise addition modulo 2 of solutions of this generator set.

become actually indistinguishable (as being present in one and the same "molecule"). We call them *congruent* (under median reflection). We give a general definition for this concept.

Definition 5. (a) Two BDPs are *congruent* if one can be transformed into the other by one of the D_3^G-symmetry operations. Otherwise they are *incongruent*. (In other terms: two BDPs are congruent if they belong to the same orbit under action of the group D_3^G.)

(b) A BDP in a given symmetry class (palindromic, rotational, dihedral) will be called *strict* (in that symmetry class), when it does not also belong to another symmetry class.

We will now derive the number of incongruent BDPs in the distinct symmetry classes, i.e. the minimal number of BDPs that generate the complete set of BDPs in a given symmetry class under D_3^G-operations.

The results from the previous Section 4.4 allow the following subset characterization. Let $\mathscr{P}_T$, $\mathscr{P}_R$, $\mathscr{P}_L$ denote the sets of BDPs that have a palindromic sequence at the top-, right- and left-edge respectively. Let $\mathscr{D}$ be the set of D_3^G-symmetric BDPs. Recall Property 14 stating that if a BDP has more than one palindromic edge, it must have dihedral symmetry, i.e., belong to $\mathscr{D}$. Thus, we can write

$$\mathscr{D} = \mathscr{P}_T \cap \mathscr{P}_R = \mathscr{P}_T \cap \mathscr{P}_L = \mathscr{P}_R \cap \mathscr{P}_L = \mathscr{P}_T \cap \mathscr{P}_R \cap \mathscr{P}_L.$$

Denoting by $\mathscr{R}$ the set of rotationally invariant BDPs, we also have $\mathscr{D} \subset \mathscr{R}$. Define the mutually disjoint sets $s\mathscr{P}_T$, $s\mathscr{P}_R$, $s\mathscr{P}_L$ and $s\mathscr{R}$ as the sets of BDPs that exhibit a strict symmetry, i.e.

$$s\mathscr{P}_T = \mathscr{P}_T \setminus \mathscr{D}, \quad s\mathscr{P}_R = \mathscr{P}_R \setminus \mathscr{D}, \quad s\mathscr{P}_L = \mathscr{P}_L \setminus \mathscr{D}, \quad s\mathscr{R} = \mathscr{R} \setminus \mathscr{D}.$$

Furthermore, let $\mathscr{N}S$ represent the set of nonsymmetric BDPs, i.e., those which do not belong to any of the classes above or, when $\mathscr{B}$ denotes the set of all BDPs:

$$\mathscr{N}S = \mathscr{B} \setminus [s\mathscr{P}_T \cup s\mathscr{P}_R \cup s\mathscr{P}_L \cup s\mathscr{R} \cup \mathscr{D}]. \tag{39}$$

Property 12. *Let $s\mathscr{P}_{nc}(N)$ represent the set*[2] *of* noncongruent *strict single-edge palindrome symmetric BDPs of size N; $s\mathscr{R}_{nc}(N)$ the set of noncongruent BDPs with strict rotational symmetry; $\mathscr{N}S_{nc}(N)$ the set of all noncongruent nonsymmetric BDPs; $\mathscr{B}_{nc}(N)$ the set of all noncongruent BDPs. Then their cardinalities are given by*

$$|s\mathscr{P}_{nc}(N)| = 2^{F_P(N)} - 2^{F_D(N)}, \tag{40a}$$

$$|s\mathscr{R}_{nc}(N)| = 2^{F_R(N)-1} - 2^{F_D(N)-1}, \tag{40b}$$

$$|\mathscr{N}S_{nc}(N)| = \tfrac{1}{3}[2^{N-1} - 2^{F_R(N)-1}] + 2^{F_D(N)-1} - 2^{F_P(N)-1}, \tag{40c}$$

$$|\mathscr{B}_{nc}(N)| = \tfrac{1}{3}[2^{N-1} + 2^{F_R(N)}] + 2^{F_P(N)-1}. \tag{40d}$$

Proof. Eq. (40a) follows from the fact that the strict single-edge palindromic BDP sets $s\mathscr{P}_T$, $s\mathscr{P}_R$, $s\mathscr{P}_L$ are elementwise congruent (under 120°-, 240°-rotation). Thus, one of these three sets is sufficient to generate all strict single-edge palindromic BDPs. Eq. (40a) gives the cardinality of each of these three sets.

The cardinality of $s\mathscr{R}$, the set of strict rotationally symmetric BDPs, is $|s\mathscr{R}| = 2^{F_R} - 2^{F_D}$. As the elements in this set occur in pairs which are congruent under median reflection, the number of noncongruent elements in this set is $|s\mathscr{R}|/2$. This gives (40b).

[2] Actually, a set of representatives of all orbits (equivalence classes) under the action of D_3^G in the specified symmetry class. Seen as a "physical" object however, a representative is indistinguishable of any other element in its orbit. Hence the use of "the set", with the connotation presented here.

From (39), it readily follows that the set of all nonsymmetric BDPs has cardinality

$$\begin{aligned}|\mathcal{NS}| &= |\mathcal{B}| - [|s\mathcal{R}| + |s\mathcal{P}_{\mathrm{L}}| + |s\mathcal{P}_{\mathrm{R}}| + |s\mathcal{P}_{\mathrm{T}}| + |\mathcal{D}|] \\ &= 2^N - [2^{F_R} - 2^{F_D} + 3(2^{F_P} - 2^{F_D}) + 2^{F_D}] \\ &= 2^N - 3.2^{F_P} - 2^{F_R} + 3.2^{F_D}. \end{aligned} \tag{41}$$

Congruent elements in $\mathcal{NS}$ occur in 6-tuples, and thus $|\mathcal{NS}_{\mathrm{nc}}| = \frac{1}{6}|\mathcal{NS}|$. This produces (40c).

The set of all noncongruent BDPs can now be constructed as the union of disjoint subsets of noncongruent BDPs: $\mathcal{B}_{\mathrm{nc}} = \mathcal{NS}_{\mathrm{nc}} \cup s\mathcal{R}_{\mathrm{nc}} \cup s\mathcal{P}_{\mathrm{nc}} \cup \mathcal{D}$. Hence, $|\mathcal{B}_{\mathrm{nc}}| = |\mathcal{NS}_{\mathrm{nc}}| + |s\mathcal{R}_{\mathrm{nc}}| + |s\mathcal{P}_{\mathrm{nc}}| + |\mathcal{D}|$. Substituting the proper expressions for these numbers as given in (40a)–(40c) yields (40d). □

Remark 9. The last result (40d) can also be obtained from direct application of the so-called *Orbit Counting Theorem* (also known as Burnside's Theorem [12,3]). The number of different BDPs is the number of different orbits obtained by letting the elements of the group D_3^G act on the set $\mathcal{B}$ of all BDPs. This theorem states that

$$|\mathcal{B}_{\mathrm{nc}}| = \frac{1}{|D_3^G|} \sum_{g \in D_3^G} |\mathcal{B}_g|$$

(of course all items considered for size N), where $\mathcal{B}_g$ is the set of elements of $\mathcal{B}$ that are left fixed under the operation g. We have $\mathcal{B}_{0^\circ} = \mathcal{B}$, $\mathcal{B}_{120^\circ} = \mathcal{R}$, $\mathcal{B}_{240^\circ} = \mathcal{R}$, $\mathcal{B}_{M_1} = \mathcal{P}_T$, $\mathcal{B}_{M_3} = \mathcal{P}_R$, $\mathcal{B}_{M_2} = \mathcal{P}_L$. This gives $|\mathcal{B}_{\mathrm{nc}}(N)| = \frac{1}{6}[2^N + 3.2^{F_P(N)} + 2^{F_R(N)}]$, which corresponds to (40d).

5. △-BDPs and the Pascal matrix transforms $P^{\nearrow}, P^{\searrow}, P^{>}, P^{<}$

5.1. △-BDPs

Consider an odd-sized BDP [see Fig. 12(a)]. It has an equilateral middle-triangular part that is *not* a BDP in the strict sense: the local BDP connection-rule is still present, but its orientation has changed by a 60°-rotation with respect to the triangle edges. It looks as if a binary difference pattern is developed starting from a vertex towards the opposite edge. We will call such a pattern a △-BDP (referring to the △-shape of its triangular support). Such a pattern is completely determined by two of its edges, for example ***a*** and ***b***, as shown in Fig. 12(b). The pattern can then indeed be grown in an unambiguous way by applying the local configuration rule, starting from cells $a(N-1)$ and $b(0)$, and evolving in the direction of the opposite edge ***c***. The rest of the paper will deal with △-BDP-symmetries.

Notice that the vertex cells themselves do not at all influence or are influenced by the rest of the pattern. For convenience, we will further delete them: △-BDP-triangles have

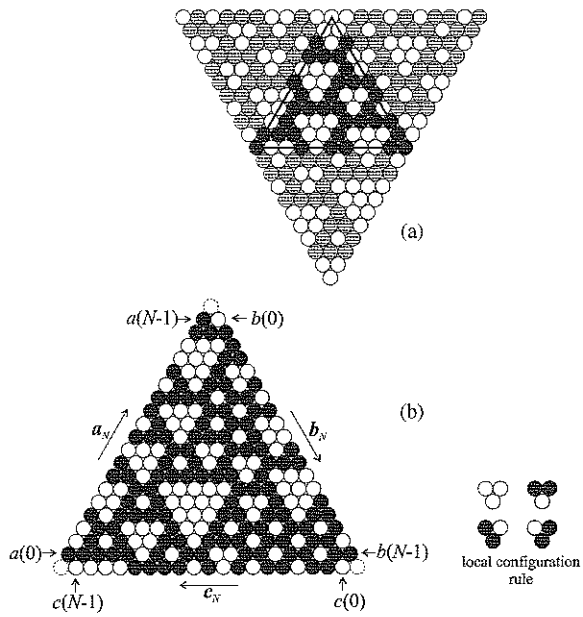


Fig. 12. (a) The whole pattern is a BDP, its middle-triangular part (highlighted) is a △-BDP. (b) The proper notation for size and orientation of △-BDP-edges.

their vertex-cells removed. Size and orientation of the edge-sequence vectors are shown in Fig. 12(b). N-sized △-BDPs actually correspond to a nonvertex-removed-triangle of size $N_{\triangle} = N + 2$. But we will keep speaking about a △-BDP of size N. Whereas there are 2^N BDPs of size N, there are 2^{2N} △-BDPs of the same size.

We need to express the bottom-edge sequence $\boldsymbol{c}$ (Fig. 12(b)) as a function of the side-edge sequences $\boldsymbol{a}$ and $\boldsymbol{b}$.

Property 13.

$$\boldsymbol{c} = P^{\searrow}\boldsymbol{a} + P^{\nearrow}\boldsymbol{b}. \tag{42}$$

Proof. First, extend the left and right edges of the △-BDP to the left and to the right, using the local matching rule [see Fig. 13(a)]. This actually imbeds the △-BDP in a regular BDP whose top edge consists of the concatenation of two N-sized sequences $\boldsymbol{l}$ and $\boldsymbol{r}$, as indicated in the figure.

The left and right triangular extensions are regular BDPs, and hence

$$\boldsymbol{r} \overset{(14)}{=} P\boldsymbol{b}, \quad \text{and} \quad \boldsymbol{l} \overset{(14)}{=} P^{\vee}\boldsymbol{a}. \tag{43}$$

Observe that the elements of $\boldsymbol{c}$ can be written as a function of the elements in $\boldsymbol{l}$ and $\boldsymbol{r}$, using (9) and (10), as

$$\boldsymbol{c} = Q\begin{bmatrix} \boldsymbol{r} \\ \boldsymbol{l} \end{bmatrix}, \tag{44}$$

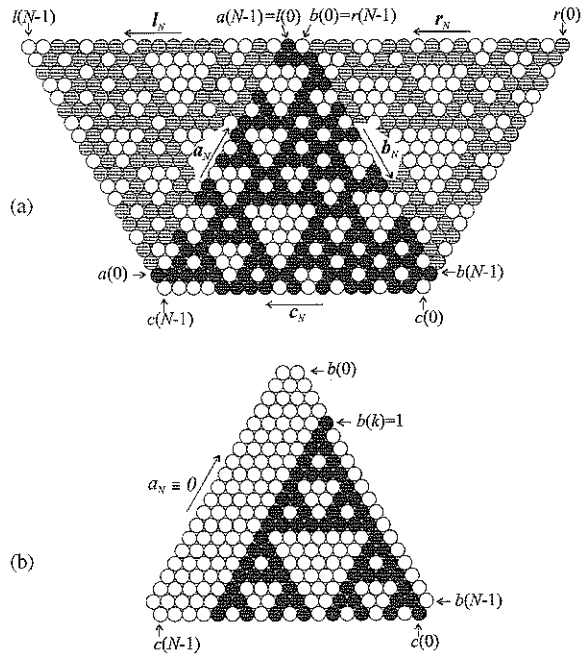


Fig. 13. (a) Expanding a △-BDP with regular BDPs. (b) The Pascal Triangular Pattern in a △-BDP with a single black cell in the $\boldsymbol{a}, \boldsymbol{b}$-edges.

where Q is the $N \times 2N$ band matrix obtained from p_{N+1}, the top row vector of size $N+1$ in the Pascal matrix P_{N+1}, as given by

$$Q = \left[\begin{array}{ccccccc|ccccccc} [1 & \cdots & \cdots & \overset{p_{N+1}}{\leftrightarrow} & \cdots & \cdots & & 1] & 0 & 0 & 0 & \cdots & 0 \\ 0 & [1 & \cdots & \cdots & \overset{p_{N+1}}{\leftrightarrow} & \cdots & & \cdots & 1] & 0 & 0 & \cdots & 0 \\ 0 & 0 & [1 & \cdots & \cdots & \overset{p_{N+1}}{\leftrightarrow} & & \cdots & \cdots & 1] & 0 & \cdots & 0 \\ \vdots & \vdots & & \ddots & & \ddots & & \ddots & & & \ddots & & \vdots \\ 0 & \cdots & 0 & 0 & 0 & [1 & & \cdots & \cdots & \overset{p_{N+1}}{\leftrightarrow} & \cdots & \cdots & 1] \\ \multicolumn{6}{c}{\underbrace{\qquad\qquad\qquad}_{Q_1}} & & \multicolumn{6}{c}{\underbrace{\qquad\qquad\qquad}_{Q_2}} \end{array}\right]. \tag{45}$$

Partitioning the Q-matrix in two $N \times N$ blocks as indicated, (44) can be rewritten as

$$\begin{aligned} \boldsymbol{c} &= Q_1\boldsymbol{r} + Q_2\boldsymbol{l} \\ &\overset{(43)}{=} Q_1P\boldsymbol{b} + Q_2P^{\vee}\boldsymbol{a} \\ &= S_1\boldsymbol{a} + S_2\boldsymbol{b}, \end{aligned} \tag{46}$$

where

$$S_1 \overset{\text{def}}{=} Q_2P^{\vee} \quad \text{and} \quad S_2 \overset{\text{def}}{=} Q_1P. \tag{47}$$

We will first show that $S_2 = P^{\nearrow}$: It will be convenient for a while to display the problem size N explicitly. So, let $\boldsymbol{a}_N \equiv 0$ and $\boldsymbol{b}_N = \boldsymbol{b}_{N,k}$, where $\boldsymbol{b}_{N,k}$, $0 \leqslant k \leqslant N-1$ is an N-vector full of zeroes, except for the single element $b_{N,k}(k) = 1$. The corresponding $\triangle$-BDP shows a Pascal's triangle modulo 2, as shown in Fig. 13(b). It means that the corresponding $\boldsymbol{c}_{N,k}$-vector is given by

$$\boldsymbol{c}_{N,k} = [p_{N-k}|0_k]^{\mathrm{T}}, \tag{48}$$

where p_{N-k} is the top row of the Pascal matrix P_{N-k}, and 0_k is a sequence of k zeroes. ($[\,]^{\mathrm{T}}$ indicates transposition ($\boldsymbol{c}$ is a column vector!).) For this particular configuration, (46) becomes

$$\boldsymbol{c}_{N,k} = S_{2,N}\boldsymbol{b}_{N,k} \quad \text{for all } k\text{: } 0 \leqslant k \leqslant N-1.$$

Constructing a matrix whose columns are the distinct $\boldsymbol{c}_{N,k}$-vectors, the last equation can be rewritten as

$$[\boldsymbol{c}_{N,0}|\boldsymbol{c}_{N,1}|\cdots|\boldsymbol{c}_{N,N-1}] = S_{2,N}[\boldsymbol{b}_{N,0}|\boldsymbol{b}_{N,1}|\cdots|\boldsymbol{b}_{N,N-1}], \tag{49}$$

or, with (48) and the definition of $\boldsymbol{b}_{N,k}$ as given above:

$$P_N^{\nearrow} = S_{2,N}I_N = S_{2,N}. \tag{50}$$

We now prove that $S_1 = P^{\searrow}$: First observe from their definitions above, that $Q_2 = Q_1^{\vee}$. Then

$$S_1 \overset{(47)}{=} Q_2P^{\vee} = Q_1^{\vee}P^{\vee} \overset{(2f,1)}{=} (Q_1^{\rightarrow}P^{\uparrow})^{\vee} \overset{(2e)}{=} (Q_1^{\rightarrow}I^{\uparrow}P)^{\vee} \overset{(2a)}{=} (Q_1P)^{\vee} \overset{(47)}{=} S_2^{\vee} \overset{(50,1)}{=} P^{\searrow}. \tag{51}$$

Taking (47), (50) and (51) together finally produces (42). □

Remark 10. Because of the linearity of the local matching rule, a $\triangle$-BDP for a given $\boldsymbol{a}$, $\boldsymbol{b}$-configuration is the cellwise sum modulo 2 of all Pascal triangular patterns like the one shown in Fig. 13(b) that propagate from the black cells in $\boldsymbol{a}$ and $\boldsymbol{b}$. That is the interpretation of Eq. (42) at the level of edge $\boldsymbol{c}$.

5.2. Product properties of the Pascal matrix transforms $P^{\nearrow}, P^{<}, P^{>}, P^{\searrow}$

Property 14. $D_3^{P_{\hat{R}}} \overset{\text{def}}{=} \langle I, I^{\uparrow}, P^{\nearrow}, P^{<}, P^{>}, P^{\searrow}; \times_{\text{mod }2}\rangle$ *forms a* D_3*-group. Its Cayley-table is*

	I	$I^{\uparrow}$	$P^{\nearrow}$	$P^{<}$	$P^{>}$	$P^{\searrow}$
I	I	$I^{\uparrow}$	$P^{\nearrow}$	$P^{<}$	$P^{>}$	$P^{\searrow}$
$I^{\uparrow}$	$I^{\uparrow}$	I	$P^{<}$	$P^{\nearrow}$	$P^{\searrow}$	$P^{>}$
$P^{\nearrow}$	$P^{\nearrow}$	$P^{>}$	$P^{\searrow}$	$I^{\uparrow}$	$P^{<}$	I
$P^{<}$	$P^{<}$	$P^{\searrow}$	$P^{>}$	I	$P^{\nearrow}$	$I^{\uparrow}$
$P^{>}$	$P^{>}$	$P^{\nearrow}$	$I^{\uparrow}$	$P^{\searrow}$	I	$P^{<}$
$P^{\searrow}$	$P^{\searrow}$	$P^{<}$	I	$P^{>}$	$I^{\uparrow}$	$P^{\nearrow}$

(52)

(*Convention*: XY *is found on the intersection of row* X *and column* Y.)

Proof. This follows from the isomorphism between $\langle I, I^{\uparrow}, P^{\nearrow}, P^{<}, P^{>}, P^{\searrow}; \times_{\mathrm{mod}\,2}\rangle$ and the $D_3^{P_R}$-group (see Property 2) $\langle I, I^{\uparrow}, P, P^{\rightarrow}, P^{\uparrow}, P^{\vee}; \times_{\mathrm{mod}\,2}\rangle$ under matrix transposition (operation $\nearrow$). Indeed, as can easily be verified from (1):

$$I^{\nearrow} = I,\ (I^{\uparrow})^{\nearrow} = I^{\uparrow}, (P)^{\nearrow} = P^{\nearrow},\ (P^{\vee})^{\nearrow} = P^{\searrow},\ (P^{\uparrow})^{\nearrow} = P^{>},\ (P^{\rightarrow})^{\nearrow} = P^{<},$$

while $(AB)^{\nearrow} \overset{(2g)}{=} B^{\nearrow}A^{\nearrow}$.

The reversal of the matrix order in this last expression implies that the Cayley-table for $D_3^{P_{\bar{R}}}$ corresponds to the *transposed* Cayley-table of $D_3^{P_R}$ [see (16)] after the substitution

$$P \mapsto P^{\nearrow},\quad P^{\uparrow} \mapsto P^{>},\quad P^{\rightarrow} \mapsto P^{<},\quad P^{\vee} \mapsto P^{\searrow}. \qquad \square$$

The following forms the counterpart of Corollary 1, and completes the set of particular properties for the D_4^G-transforms of the Pascal matrix.

Corollary 3.

$$(P^{\nearrow})^3 = (P^{\searrow})^3 = (P^{>})^2 = (P^{<})^2 = I, \tag{53a}$$

$$(P^{\nearrow})^2 = P^{\searrow},\quad (P^{\searrow})^2 = P^{\nearrow}. \tag{53b}$$

Remark 11. The group $D_3^{P_{\bar{R}}}$ is isomorphic with the D_3^G-group of geometric operations under the one-to-one mapping

$$\mathscr{G}'\colon\ R_{0^\circ} \mapsto I,\ R_{120^\circ} \mapsto P^{\nearrow},\ R_{240^\circ} \mapsto P^{\searrow},\ M_1 \mapsto I^{\uparrow},\ M_2 \mapsto P^{<},\ M_3 \mapsto P^{>}.$$

Compare this with its counterpart (17). Again there is an analytic-geometric interpretation of this isomorphism. It is illustrated in Fig. 14, which is similar to Fig. 6, except that we now consider the *bottom-edge* sequences of the $\triangle$-BDPs, and the expressions relating them to the corresponding side-edge sequences. Let $\mathscr{U}^{\triangle} = \{A, B, C, D, E, F\}$ be the set of $\triangle$-BDPs displayed in Fig. 14, and let $\mathscr{L} = \{\boldsymbol{c}, \boldsymbol{b}^{\uparrow}, \boldsymbol{a}, \boldsymbol{a}^{\uparrow}, \boldsymbol{b}, \boldsymbol{c}^{\uparrow}\}$ be the set of the corresponding bottom-edge sequences. With $\boldsymbol{x} \in \mathscr{L}$, denote by $F(\boldsymbol{x})$ the following expression:

$$F(\boldsymbol{x}) \equiv \boldsymbol{x} + P^{\searrow}\boldsymbol{x}_{\mathrm{L}} + P^{\nearrow}\boldsymbol{x}_{\mathrm{R}} = 0, \tag{54}$$

(being equivalent to $\boldsymbol{x} = P^{\searrow}\boldsymbol{x}_{\mathrm{L}} + P^{\nearrow}\boldsymbol{x}_{\mathrm{R}}$ in $\mathbb{F}_2$), which relates the bottom-edge sequence $\boldsymbol{x}$ of a $\triangle$-BDP to the corresponding left- and right-side edge sequences $\boldsymbol{x}_{\mathrm{L}}$ and $\boldsymbol{x}_{\mathrm{R}}$ as shown in Fig. 14. For example, when $\boldsymbol{x} = \boldsymbol{c}^{\uparrow}$ (bottom sequence of $\triangle$-BDP F in Fig. 14), $F(\boldsymbol{c}^{\uparrow}) \equiv \boldsymbol{c}^{\uparrow} + P^{\searrow}\boldsymbol{b}^{\uparrow} + P^{\nearrow}\boldsymbol{a}^{\uparrow} = 0$ (see (42)).

Expression $F(\boldsymbol{x})$ in (54) will also be considered equivalent to the one in which $\boldsymbol{x}, \boldsymbol{x}_{\mathrm{L}}, \boldsymbol{x}_{\mathrm{R}}$ in it are expressed as $I^{\uparrow}\boldsymbol{x}^{\uparrow}, I^{\uparrow}(\boldsymbol{x}_{\mathrm{L}})^{\uparrow}, I^{\uparrow}(\boldsymbol{x}_{\mathrm{R}})^{\uparrow}$, respectively, yielding $I^{\uparrow}\boldsymbol{x}^{\uparrow} + P^{<}(\boldsymbol{x}_{\mathrm{L}})^{\uparrow} + P^{>}(\boldsymbol{x}_{\mathrm{R}})^{\uparrow} = 0$ (using (52)).

Define $\mathscr{F} = F(\mathscr{L}) = \{F(\boldsymbol{c}), F(\boldsymbol{b}^{\uparrow}), F(\boldsymbol{a}), F(\boldsymbol{a}^{\uparrow}), F(\boldsymbol{b}), F(\boldsymbol{c}^{\uparrow})\}$, i.e., the set of expressions displayed in Fig. 14.

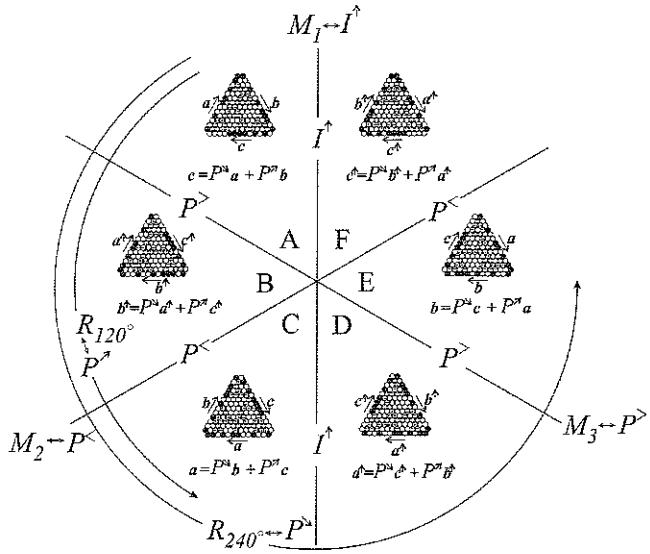


Fig. 14. "Analytic-geometric" interpretation of the isomorphism $\mathscr{G}' : \langle R_{0^\circ}, R_{120^\circ}, R_{240^\circ}, M_1, M_2, M_3; \circ \rangle \to \langle I, P^{\nearrow}, P^{\searrow}, I^{\uparrow}, P^{<}, P^{>}; \times_{\mathrm{mod}\,2} \rangle$. The expressions transform into each other by the proper matrix multiplications.

The action $\phi_{D_3^G, \mathscr{U}^{\triangle}} : D_3^G \times \mathscr{U}^{\triangle} \to \mathscr{U}^{\triangle} : (g, \boldsymbol{x}) \mapsto g(\boldsymbol{x})$, as illustrated in Fig. 14 (in a similar way as was done in Fig. 5 for "regular" BDPs), induces a "geometric" action on $\mathscr{F}$, as follows:

$$\phi_{D_3^G, \mathscr{F}} : D_3^G \times \mathscr{F} \to \mathscr{F} : (g, F(\boldsymbol{x})) \mapsto F(g(\boldsymbol{x}))$$
$$\equiv g(\boldsymbol{x}) + P^{\searrow}(g(\boldsymbol{x}))_L + P^{\nearrow}(g(\boldsymbol{x}))_R = 0$$

(because $(h \circ g, F(\boldsymbol{x})) = F(h \circ g(\boldsymbol{x})) = F(h(g(\boldsymbol{x})) = (h, F(g(\boldsymbol{x})))$ for all $h, g \in D_3^G$ and all $\boldsymbol{x} \in \mathscr{L}$).

On the other hand, the mapping

$$\phi_{D_3^{P_{\bar{R}}}, \mathscr{F}} : D_3^{P_{\bar{R}}} \times \mathscr{F} \to \mathscr{F} : (W, F(\boldsymbol{x})) \mapsto WF(\boldsymbol{x}) \equiv W\boldsymbol{x} + WP^{\searrow}\boldsymbol{x}_L + P^{\nearrow}\boldsymbol{x}_R = 0$$

defines an "analytic" action on $\mathscr{F}$ (because $(W_1 W_2, F(\boldsymbol{x})) \mapsto W_1 W_2 F(\boldsymbol{x}) \equiv W_1 W_2 + W_1 W_2 P^{\searrow}\boldsymbol{x}_L + W_1 W_2 P^{\nearrow}\boldsymbol{x}_R = 0$, this last expression being identical to $W_1(W_2 F(\boldsymbol{x}))$). The fact that D_3^G and $D_3^{P_{\bar{R}}}$ are isomorphic induces an isomorphism between both their actions on $\mathscr{F}$ [14] (and actually also between both of them and the action of D_3^G on $\mathscr{L}$), implying that for all $g, h \in D_3^G$ and for all $\boldsymbol{x} \in \mathscr{L}$, we have

$$g(F(\boldsymbol{x})) = F(g(\boldsymbol{x})) = \mathscr{G}'(g) F(\boldsymbol{x}), \tag{55}$$

$$(h \circ g)(F(\boldsymbol{x})) = F(h \circ g(\boldsymbol{x})) = \mathscr{G}'(h \circ g) F(\boldsymbol{x}) = \mathscr{G}'(h)\mathscr{G}'(g) F(\boldsymbol{x}). \tag{56}$$

For example, with $g = R_{240^\circ}$, $h = M_3$ and $\boldsymbol{x} = \boldsymbol{c}^{\uparrow}$, we find for the geometric action

$$(M_3 \circ R_{240^\circ}) F(\boldsymbol{c}^{\uparrow}) = F(M_2 \boldsymbol{c}^{\uparrow}) = F(\boldsymbol{b}).$$

Under the isomorphism, this becomes

$$\mathscr{G}'(M_3 \circ R_{240^\circ})F(\boldsymbol{c}^\uparrow) = \mathscr{G}'(M_3)\mathscr{G}'(R_{240^\circ})F(\boldsymbol{c}^\uparrow) = P^{>}P^{\searrow}F(\boldsymbol{c}^\uparrow)$$
$$\overset{(52)}{=} P^{<}F(\boldsymbol{c}^\uparrow) \equiv P^{<}\boldsymbol{c}^\uparrow + P^{<}P^{\searrow}\boldsymbol{b}^\uparrow + P^{<}P^{\nearrow}\boldsymbol{a}^\uparrow = 0.$$

The last expression is also $F(\boldsymbol{b})$, as it equals $P^{<}\boldsymbol{c}^\uparrow + I^\uparrow\boldsymbol{b}^\uparrow + P^{>}\boldsymbol{a}^\uparrow = 0$ (or $\boldsymbol{b} + P^{\searrow}\boldsymbol{c} + P^{\nearrow}\boldsymbol{a} = 0$).

6. △-BDPs with particular symmetries

6.1. △-BDPs with palindrome (S_2^G) symmetry

Property 15. *Necessary and sufficient for a △-BDP to have palindrome symmetry (reflection symmetry about the vertical median), is that* $\boldsymbol{a}^\uparrow = \boldsymbol{b}$.

Proof. (a) The necessary part is obvious.

(b) *Sufficient part*: For an M-sized △-BDP, $\boldsymbol{a}_M^\uparrow = \boldsymbol{b}_M$ implies that $\boldsymbol{c}_M = \boldsymbol{c}_M^\uparrow$. Indeed,

$$\boldsymbol{c}_M \overset{(42)}{=} P^{\searrow}\boldsymbol{a}_M + P^{\nearrow}\boldsymbol{b}_M = P^{\searrow}\boldsymbol{b}_M^\uparrow + P^{\nearrow}\boldsymbol{a}_M^\uparrow \overset{\text{Fig. 14}}{=} \boldsymbol{c}_M^\uparrow. \tag{57}$$

Start now with an N-sized △-BDP for which $\boldsymbol{a}_N^\uparrow = \boldsymbol{b}_N$, and thus $\boldsymbol{c}_N = \boldsymbol{c}_N^\uparrow$. Consider the sub-△-BDPs of size M, $2 \leqslant M \leqslant N$ with the same top as the original △-BDP. Then (57) holds for all these sub-△-BDPs, implying that all sequences of the original △-BDP that are parallel to the $\boldsymbol{c}_N$-edge are palindromic. □

Remark 12. In contrast to the regular BDP-case, the condition $\boldsymbol{c}=\boldsymbol{c}^\uparrow$ does not necessarily imply that $\boldsymbol{a}^\uparrow=\boldsymbol{b}$ (or that the corresponding △-BDP exhibits palindrome symmetry). For example, $\boldsymbol{a}=100110$ and $\boldsymbol{b}=010111$ produce the palindrome $\boldsymbol{c}=101101$, although $\boldsymbol{a}^\uparrow \neq \boldsymbol{b}$.

The following is a rather trivial consequence of the previous property.

Corollary 4. *The number of palindrome-symmetric △-BDPs of size N is* 2^N, *or: the number of degrees of freedom is*

$$F_P^{\triangle}(N) = N. \tag{58}$$

Remark 13. Observe that $F_P^{\triangle}(N) = F_P(2N)$. This is so because there is a one-to-one correspondence between palindromic △-BDPs of size N and palindromic BDPs of size $2N$, the first being the middle triangular parts of the last ones (recall Fig. 12, keeping in mind that the vertex cells are not considered in △-BDPs). As another consequence of this, Property 5(b) implies that all △-BDP cells that lie *on* the median perpendicular to the palindromic edge must be white.

6.2. △-BDPs with rotational ($\langle R_{120^\circ}\rangle$) symmetry

It is clear that here also a necessary and sufficient condition for rotational symmetry is given by the condition $\boldsymbol{a}=\boldsymbol{b}=\boldsymbol{c}$ (because two edges completely determine the third edge). Thus, all three edge-sequences must be equal, and it makes sense to speak about "the" edge-sequence of a rotationally symmetric △-BDP.

Property 16. (a) *$\boldsymbol{a}$ is the edge-sequence of a rotationally symmetric △-BDP if and only if it satisfies the equation*

$$[I+P^{\searrow}+P^{\nearrow}]\boldsymbol{a}=0. \tag{59}$$

(b) *The number of rotationally symmetric △-BDPs of size N is given by $2^{F_R^{\triangle}(N)}$, with the number of degrees of freedom*

$$F_R^{\triangle}(N)=F_R(2N)=2\left\lfloor\frac{N+1}{3}\right\rfloor. \tag{60}$$

Proof. (a) Follows from applying the condition $\boldsymbol{a}=\boldsymbol{b}=\boldsymbol{c}$ to Eq. (42).

(b) Expanding a given N-sized △-BDP with $\boldsymbol{a}=\boldsymbol{b}=\boldsymbol{c}$ to a regular BDP of size $2N$ (refer to Fig. 12(a) again), shows that this BDP is unique and has also rotational symmetry. On the other hand, each $2N$-sized rotationally symmetric BDP has a unique rotationally symmetric △-BDP of size N as its middle triangular part. Thus, there is a one-to-one correspondence between rotationally symmetric BDPs of size $2N$ and rotationally symmetric △-BDPs of size N, and this implies the first equality of (60). The second equality follows from evaluating (26) by substituting $2N$ for N. □

Remark 14.

- Solving the set of Eqs. (59), for example by reducing it to row echelon form, produces $F_R^{\triangle}(N)$ free variables. Again, all solutions form a group under cellwise addition modulo 2 (isomorphic to the free-variable configuration set).
- Observe that, as opposed to the regular BDP case, the condition $\boldsymbol{a}=\boldsymbol{b}$ does not imply $\boldsymbol{a}=\boldsymbol{b}=\boldsymbol{c}$ (or rotational symmetry). For example $\boldsymbol{a}=\boldsymbol{b}=110111$ produces $\boldsymbol{c}=000110\neq\boldsymbol{a}$.

6.3. △-BDPs with dihedral (D_3^G) symmetry

Just as for the BDP-case dealt with in Section 4.4, a necessary and sufficient condition for dihedral symmetry is that $\boldsymbol{a}=\boldsymbol{a}^{\uparrow}=\boldsymbol{b}=\boldsymbol{c}$. In contrast, however, neither the conditions $\boldsymbol{a}=\boldsymbol{a}^{\uparrow}=\boldsymbol{b}$, nor $\boldsymbol{a}=\boldsymbol{a}^{\uparrow}\,\&\,\boldsymbol{b}=\boldsymbol{b}^{\uparrow}$ are sufficient for dihedral symmetry.

Property 17. (a) *Let $\boldsymbol{a}_{\lceil N/2\rceil}$ be the vector whose elements are the $\lceil N/2\rceil$ first elements of the edge $\boldsymbol{a}_N$ of a dihedrally symmetric △-BDP of size N, then $\boldsymbol{a}_{\lceil N/2\rceil}$ satisfies the equation*

$$[T_1+T_2^{\rightarrow}]\boldsymbol{a}_{\lceil N/2\rceil}=0, \tag{61}$$

where T_1 and T_2 are obtained from the $[T_1|T_2']$ partitioning of the matrix $[I+P^{\searrow}+P^{\nearrow}]$ into two blocks of $\lceil N/2\rceil$ and $N-\lceil N/2\rceil$ columns, respectively, and where $T_2=T_2'$ if N is even, and $T_2=[0|T_2']$ if N is odd (T_2' augmented with one column of 0s). The other elements of $\boldsymbol{a}_N$ follow from the reflective symmetry condition

$$a(N-k-1)=a(k) \quad \text{for } k\leqslant\left\lceil\frac{N}{2}\right\rceil. \tag{62}$$

Conversely, any solution of equations (61)–(62) produces the edge sequence of a dihedrally symmetric BDP.

(b) *The number of dihedrally-symmetric $\triangle$-BDPs of size N is $2^{F_D^{\triangle}(N)}$, with the number of degrees of freedom*

$$F_D^{\triangle}(N)=F_D(2N)=\left\lfloor\frac{2N+3}{6}\right\rfloor. \tag{63}$$

Proof. (a) Eq. (61) is a straightforward reduction of the rotational symmetry condition (59) under the additional palindromic condition $\boldsymbol{a}=\boldsymbol{a}^{\uparrow}$. The converse statement in (a) follows from reversing the argumentation showing that (61) is equivalent to $[I+P^{\searrow}+P^{\nearrow}]\boldsymbol{a}=0$, with $\boldsymbol{a}=\boldsymbol{a}^{\uparrow}$.

(b) Is again a consequence of the argument that there is a one-to-one correspondence between D_3^G-symmetric $\triangle$-BDPs of size N and their expanded regular BDPs of size $2N$ that are also D_3^G-symmetric. The second equation follows from evaluating (30) when N is replaced by $2N$. □

6.4. Incongruent $\triangle$-BDPs

Congruence and incongruence of $\triangle$-BDPs are defined in the same way as for BDPs (see Section 4.5), and because of the one-to-one correpondence between $\triangle$-BDPs of size N and BDPs of size $2N$ with identical symmetries, we find the same expressions for the number of noncongruent $\triangle$-BDPs in the different symmetry classes, except for the fact that the degrees of freedom-number $F_*(N)$ should be replaced by $F_*^{\triangle}(N)=F_*(2N)$. This produces the $\triangle$-BDP-counterpart of Property 12:

Property 18. *Let $s\mathscr{P}_{nc}^{\triangle}(N)$ represent the set (see footnote 2) of* noncongruent *strict single-edge palindrome symmetric $\triangle$-BDPs; $s\mathscr{R}_{\mathrm{nc}}^{\triangle}(N)$ the set of noncongruent $\triangle$-BDPs with strict rotational symmetry; $\mathscr{N}S_{\mathrm{nc}}^{\triangle}(N)$ the set of all noncongruent nonsymmetric $\triangle$-BDPs; $\mathscr{B}_{\mathrm{nc}}^{\triangle}(N)$ the set of all noncongruent $\triangle$-BDPs. Then their cardinalities are given by*

$$|s\mathscr{P}_{\mathrm{nc}}^{\triangle}(N)|=2^{F_P^{\triangle}(N)}-2^{F_D^{\triangle}(N)}, \tag{64a}$$

$$|s\mathscr{R}_{\mathrm{nc}}^{\triangle}(N)|=2^{F_R^{\triangle}(N)-1}-2^{F_D^{\triangle}(N)-1}, \tag{64b}$$

$$|\mathscr{N}S_{\mathrm{nc}}^{\triangle}(N)|=\tfrac{1}{3}[2^{2N-1}-2^{F_R^{\triangle}(N)-1}]+2^{F_D^{\triangle}(N)-1}-2^{F_P^{\triangle}(N)-1}, \tag{64c}$$

$$|\mathscr{B}_{\mathrm{nc}}^{\triangle}(N)|=\tfrac{1}{3}[2^{2N-1}+2^{F_R^{\triangle}(N)}]+2^{F_P^{\triangle}(N)-1}. \tag{64d}$$

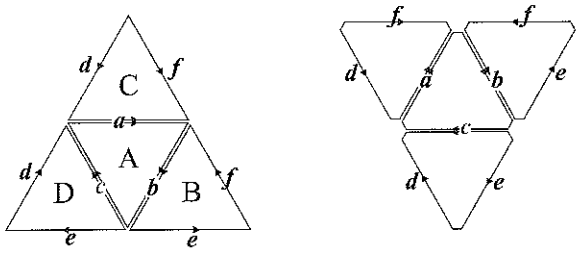


Fig. 15. Edge-configurations for the unfolded faces of edge-fitting BDP- and △-BDP-covered tetrahedra.

7. BDP- and △-BDP-covered tetrahedra

As an application inspired from decorative mathematical artwork [17,18], we wonder what kind of BDPs (or △-BDPs) would fit on the faces of a regular tetrahedron, taking into account that each edge-sequence of the tetrahedron is common to two distinct faces. Such a covering of a tetrahedron with (△-)BDPs will be called *edge-fitting*. A face of the tetrahedron will be identified with its covering BDP.

Property 19. *An edge-fitting BDP-covered tetrahedron has identical dihedrally symmetric faces.*

Proof. Consider Fig. 15(a), showing the four faces of an unfolded tetrahedron and indicating the edge-sequences already satisfying the edge-fitting condition. Start with a BDP on face A. As all other faces are also BDPs, we find that

In face B: $\boldsymbol{f}=\boldsymbol{a}$, $\boldsymbol{e}=\boldsymbol{c}^{\uparrow}$ ($\boldsymbol{b}$ being common to faces A and B).

In face C: $\boldsymbol{f}=\boldsymbol{b}^{\uparrow}, \boldsymbol{d}=\boldsymbol{c}^{\uparrow}$ ($\boldsymbol{a}$ being common to faces A and C).

In face D: $\boldsymbol{d}=\boldsymbol{a}$, $\boldsymbol{e}=\boldsymbol{b}$ ($\boldsymbol{e}$ being common to faces A and D).

It follows that $\boldsymbol{a}=\boldsymbol{f}=\boldsymbol{d}=\boldsymbol{c}^{\uparrow}=\boldsymbol{e}=\boldsymbol{b}=\boldsymbol{b}^{\uparrow}$, and because of the last equality $\boldsymbol{b}=\boldsymbol{b}^{\uparrow}$, it also follows that all edges are identical palindromic sequences, and this implies the truth of the assertion. □

The next property will show that more freedom is possible for △-BDP edge-fitting coverings of tetrahedra. The following property refers to the edge-sequence configuration of Fig. 15(b).

Property 20. *An edge-fitting △-BDP-covered tetrahedron is completely determined by three edges that do not form a loop. The generic possibilities are*

- *a chain of three edges, such as* $\boldsymbol{d},\boldsymbol{a},\boldsymbol{b}$. *These are solutions of the* $\mathbb{F}_2$*-equations*

$$[I+P^{>}]\boldsymbol{d}+[I+P^{<}]\boldsymbol{b}+[P^{\searrow}+P^{\nearrow}]\boldsymbol{a}=0, \tag{65}$$

- *three edges with a common vertex, such as* $\boldsymbol{a},\boldsymbol{b},\boldsymbol{f}$. *These are solutions of the* $\mathbb{F}_2$*-equations*

$$[I+P^{>}]\boldsymbol{f}+[I^{\uparrow}+P^{\searrow}]\boldsymbol{b}^{\uparrow}+[P^{\nearrow}+P^{<}]\boldsymbol{a}=0. \tag{66}$$

Proof. First, it is clear that three edges forming a loop can only determine one face (the one containing these three edges). The two other possibilities for specifying three edges are the canonical ones given above, and iterating the $\triangle$-BDP dependency (two edges in a face determine the third one) makes that these determine all edges. Apply Eq. (42) for the different faces of the tetrahedron:

$$\boldsymbol{c}\overset{(42)}{=}P^{\searrow}\boldsymbol{a}+P^{\nearrow}\boldsymbol{b}, \tag{67}$$

$$\boldsymbol{e}\overset{(42)}{=}P^{\searrow}\boldsymbol{d}+P^{\nearrow}I^{\uparrow}\boldsymbol{c}\overset{(67,52)}{=}P^{\searrow}\boldsymbol{d}+P^{<}\boldsymbol{a}+I^{\uparrow}\boldsymbol{b}, \tag{68}$$

$$\boldsymbol{f}\overset{(42)}{=}P^{\searrow}\boldsymbol{b}+P^{\nearrow}\boldsymbol{e}\overset{(68,52))}{=}[P^{\searrow}+P^{>}]\boldsymbol{b}+\boldsymbol{d}+I^{\uparrow}\boldsymbol{a}, \tag{69}$$

$$\boldsymbol{d}\overset{(42)}{=}P^{\searrow}\boldsymbol{a}+P^{\nearrow}I^{\uparrow}\boldsymbol{f}\overset{(69,52)}{=}[P^{\searrow}+P^{\nearrow}]\boldsymbol{a}+[I+P^{<}]\boldsymbol{b}+P^{>}\boldsymbol{d}. \tag{70}$$

Eq. (70) is equivalent to (65).

Once $\boldsymbol{a},\boldsymbol{b},\boldsymbol{d}$ are solved from (65), one can use Eqs. (67)–(69) in order to derive all other edge-sequences and, in fact, the complete $\triangle$-BDP-faces. Eq. (66) can be obtained from (65) by using the substitutions $\boldsymbol{d}=P^{\searrow}\boldsymbol{a}+P^{\nearrow}I^{\uparrow}\boldsymbol{f}$ and $\boldsymbol{b}=I^{\uparrow}\boldsymbol{b}^{\uparrow}$. □

Having solved the tetrahedron equations (65) for increasing problem size N has led to the following observation [8] concerning the number of free variables in the solution.

Observation 1. *The number of degrees of freedom in solving the* $\triangle$*-BDP covering problem for a tetrahedron is given by*

$$T(N)=N+\left\lceil\frac{N}{2}\right\rceil+\left\lfloor\frac{N-2}{3}\right\rfloor+(N-2)\bmod 3 +\frac{N-2-\lfloor(N-2)/3\rfloor-(N-2)\bmod 3}{2}+n_N, \tag{71}$$

where $n_N=1$ *when* $N\neq 2^k$, $k=1,2,\ldots$; $n_N=2$ *when* $N=2^k$.

Solutions of edge-fitting $\triangle$-BDP-covered tetrahedra provided by (65) do not necessarily exhibit some form of symmetry. An example is shown in Fig. 16(a). Symmetries may be enforced by additional conditions on the edges. A more extensive analysis [8] has shown that there are three main symmetry cases (some of which containing subcases of higher symmetry):

- The first case imposes the additional condition $\boldsymbol{a}=\boldsymbol{b}^{\uparrow}$ and results in two palindromic faces (not necessarily identical) with a common palindromic edge, the other two faces are mirror images of each other (but do not necessarily show any particular

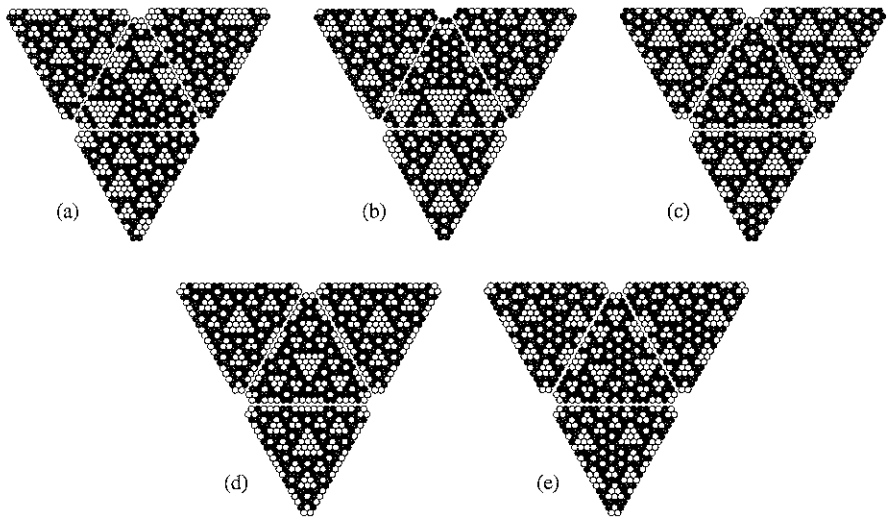


Fig. 16. Examples of △-BDP-covered tetrahedra (unfolded) with particular symmetries (△-BDP-size 19): (a) a general solution without symmetry; (b) $a = b^{\uparrow}$; (c) $a = b = c$; (d) $a = b = c = e$; (e) $a = b = d$.

symmetry). This tetrahedron is determined by the triple (a, b, d), where a and d satisfy

$$[I^{\uparrow} + P^{\nearrow}](d^{\uparrow} + a) = 0 \tag{72}$$

(this is the reduction of (65) under the additional condition). An example is shown in Fig. 16(b).

- The second case concerns the additional condition $a{=}b{=}c$. It results in a tetrahedron with one dihedrally symmetric face (the face defined by a, b, c) and three identical palindromic faces. It is completely determined by the triple (a, b, e), in which e and a satisfy

$$[I + I^{\uparrow} + P^{\searrow} + P^{\nearrow} + P^{<} + P^{>}]e = 0, \tag{73}$$

$$a = [P^{\searrow} + P^{>}]e.$$

An example is shown in Fig. 16(c).

There is an important subcase $a = b = c = e$ which enforces the highest degree of symmetry: all edges are identical palindromes, and so all △-BDP-faces are identical and dihedrally symmetric (see Fig. 16(d) for an example). The common edge, say a, satisfies

$$[I + P^{\searrow} + P^{>}]a = 0. \tag{74}$$

- The third case enforces the condition $a = b = d$, and produces four congruent faces. Edge a satisfies

$$[P^{<} + P^{>} + P^{\searrow} + P^{\nearrow}]a = 0. \tag{75}$$

An example is displayed in Fig. 16(e).

The number of solutions for these particular symmetry cases is given by $2^{T_i(N)}$, where the $T_i(N)$ are provided by the following:

Observation 2. *Denoting by T_1, T_2, T_3, T_4 the numbers of degrees of freedom in the solution of* (72), (73), (74), (75), respectively, it has been observed [8] that

$$T_1(N) = N + \left\lfloor \frac{N+1}{2} \right\rfloor, \qquad T_2(N) = \begin{cases} 5\lfloor \frac{N}{6} \rfloor + 3 & \text{if } N \bmod 6 = 4, \\ 5\lfloor \frac{N}{6} \rfloor + N \bmod 6 & \text{if } N \bmod 6 \neq 4, \end{cases}$$

$$T_3(N) = \left\lfloor \frac{N+1}{3} \right\rfloor, \qquad T_4(N) = \begin{cases} \frac{N}{3} + 1 & \text{if } N = 3k, \\ \lfloor \frac{N}{3} \rfloor + 2 & \text{if } N \neq 3k. \end{cases}$$

Acknowledgements

This work was partially supported by The Concerted Action project GOA-MIPS of the Flemish Community, and by the Belgian Program on Interuniversity Attraction Poles of the Belgian Prime Minister's Office for Science, Technology and Culture (IUAP P4-02).

References

[1] J.-P. Allouche, V. Berthé, Triangle de Pascal, complexité et automates, Bull. Belg. Math. Soc. Simon Stevin 4 (1997) 1–23.
[2] J.-P. Allouche, F. von Haeseler, H.-O. Peitgen, G. Skordev, Linear cellular automata, finite automata and Pascal's triangle, Discrete Appl. Math. 66 (1996) 1–22.
[3] M.A. Armstrong, Groups and Symmetry, Springer, New York, 1988.
[4] A. Barbé, Periodic patterns in the binary difference field, Complex Systems 2 (1988) 209–233.
[5] A. Barbé, A cellular automaton ruled by an eccentric conservation law, Physica D 45 (1990) 49–62.
[6] A. Barbé, Coarse-graining invariant orbits of one-dimensional Z_p-linear cellular automata, Internat. J. Bifurcation Chaos Appl. Sci. Eng. 6 (1996) 2237–2297.
[7] A. Barbé, Complex order from disorder and from simple order in coarse-graining invariant orbits of certain two-dimensional linear cellular automata, Internat. J. Bifurcation Chaos Appl. Sci. Eng. 7 (1997) 1451–1496.
[8] A. Barbé, Symmetric coverings of triangles with Pascal's Triangles modulo 2, SISTA/COSIC Internal Report No. 98-54, Department of Electrical Engineering, K.U.Leuven, 1998.
[9] A. Barbé, F.von Haeseler, H.-O. Peitgen, G. Skordev, Coarse-graining invariant patterns of one-dimensional two-state linear cellular automata, Internat. J. Bifurcation Chaos Appl. Sci. Eng. 5 (1995) 1611–1631.
[10] F.J. Budden, The Fascination of Groups, Cambridge University Press, Cambridge, 1972.
[11] H. Faure, H. Chaix, Minoration de discrépance en dimension 2, C. R. Acad. Sci. Paris Sér I 319 (1994) 1–4.
[12] J.A. Gallian, Contemporary Abstract Algebra, D.C. Heath and Company, Lexington, 1994.
[13] H. Gutowitz (Ed.), Cellular Automata: Theory and Experiment, A Bradford Book, MIT Press, Cambridge MA, 1991; reprinted from Physica D 45 (1–3), (1990).

[14] A. Kerber, Applied Finite Group Actions, 2nd Edition, Springer, Berlin, 1999.
[15] I. Korec, Irrational speeds of configurations growth in generalized Pascal's triangles, Theoret. Comput. Sci. 112 (1993) 399–412.
[16] H.-O. Peitgen, H. Jürgens, D. Saupe, Chaos and Fractals, Springer, New York, 1992.
[17] D. Schattschneider, Visions of Symmetry: Notebooks, Periodic Drawings, and Related Work of M.C. Escher, W.H. Freeman, New York, 1990.
[18] D. Schattschneider, W. Walker, M.C. Escher Kaleidozyklen, TACO, Berlin, 1987.
[19] S. Wolfram, Cellular Automata and Complexity, Addison-Wesley, Reading, MA, 1994.
[20] Z. Zhang, M. Liu, An extension of the generalized Pascal matrix and its algebraic properties, Linear Algebra Appl. 271 (1998) 169–177.